TOTAL PAGES : 54

HERSCHEL / PLANCK

Planck Payload Optical Performances analysis

H-P-3-ASPI-AN-0331

Product Code : 22000

Rédigé par/ *Written by*	**Responsabilité-Service-Société** ***Responsibility-Office -Company***	**Date**	**Signature**
Ph. Martin	Planck Optical Engineer	09-Apr 2004	
Vérifié par/ *Verified by*			
J.B. Riti	Planck PLM technical manager	09.04.2004	
Approbation/*Approved*			
E. POURRIER	Planck Payload PA	9/04/2004	
Th. Banos	Planck PLM manager	9/04/04	
J-J. JUILLET	Project Manager	09/04/04	

Data management : G. SERRA

Entité Emettrice : Alcatel Space - Cannes
(détentrice de l'original) :

ORGANISME

ALCATEL
SPACE

CLASSIFICATION				
Secret militaire		**Secret industriel**		
NC DR CD SD ☒ ☐ ☐ ☐		**NC RA CA SA** ☒ ☐ ☐ ☐		
MARCHE ou CONTRAT				
Numéro du marché ou du contrat		Organisme client		
Contractuel Npn	Programme HERSCHEL-PLANCK	Lot NA	Poste NA	LT. FC22-ADF

TITRE

Planck Payload
Optical Performances Analysis

AUTEUR (S) (Personne physique) Ph. MARTIN

Date	Numéro d'origine du document		Nombre			
(JJ - MM - AA)	**H-P-3-ASPI-AN-0331**		Pages	Figures	Annexes	Réf. Biblio
09-Apr-2004	**Ed. 02**	**Rév. 0**	**54**	**/**	**/**	**/**

RESUME D'AUTEUR
Ce document présente l'analyse des performances optiques de la charge utile Planck. Elle couvre:
Le besoin de qualité image (WFE)
Le besoin de ligne de visée
Le besoin d'émissivité

Support Informatique
Réf. disquette ou fichier
NA

Catégorie de diffusion

2			D	
3	x		I	x

Mots Clés
Planck; Telescope; performances optiques;

Service : OS/I/IO
Nom : L.BOULISSIERE
Signature :

Département : OS/I/I
Nom : JA. MASSONI
Signature :

HERSCHEL/PLANCK	**DISTRIBUTION RECORD**
DOCUMENT NUMBER : H-P-3-ASPI-AN-0331	Issue: 02/ Rev. : 00 Date: 09-Apr-2002

EXTERNAL DISTRIBUTION		**INTERNAL DISTRIBUTION**	
ESA	**X**	**HP team**	**X**
ASTRIUM			
ALENIA			
CONTRAVES			
TICRA			
TECNOLOGICA			
		Clt Documentation	**Orig.**

ENREGISTREMENT DES EVOLUTIONS / *CHANGE RECORDS*

ISSUE	DATE	§ : DESCRIPTION DES EVOLUTIONS *§ : CHANGE RECORD*	REDACTEUR *AUTHOR*
1.0	28-Jun-2002	PDR First issue	Ph. MARTIN
2.0	09 Apr 2004	Planck PLM CDR update Includes -reflectors QM shape mechanical measurement -reflectors FEM results -structure and cryostructure CDR results	Ph. MARTIN

TABLE OF CONTENTS

1. SCOPE

This documents contains the Planck Payload Optical performances analysis.

The optical performances of the Planck Telescope are Wave Front Error, Line of sight position and stability, and reflectors emissivity.

The present document, is an update of the PDR analyses, study, taking particularly into account

- Structure knowledge as per CSAG analysis
- Reflectors QM knowledge as per ESA/ASED documentation and measurements

LoS requirements, derived from ACMS needs in the Planck Alignment Plan are analyzed

The low emissivity performance, as requested in the "Planck Telescope design specification" (cf [AD1]) is analyzed in the document, as it is considered as an optical performance.

APPLICABLE AND REFERENCE DOCUMENTS

2.1 Applicable documents

[AD1] " Planck telescope optical and RF system specification "
H-P-3-ASP-SP-0274 issue 1. Date of issue: 01-Juil-2002.

[AD2] " Primary reflector / secondary reflector specification "
SCI-PT-RS-07422. Issue 5 Revision 2. Date of issue: 08-Aug-2003.

[AD3] System Requirement Specification "
SCI-PT-RS-05911. Issue 3 Revision 2. Date of issue: 01-Dec-2003.

[AD4] Instrument Interface Document
SCI-PT-IIDA-04624 Issue 3.1

[AD5] " Planck PLM optical analysis – inputs for WFE and Gain budgets"
H-P-3-ASP-AN-0742 Issue 1 Revision 0. Date of issue: Apr 2004.

2.2 Reference documents

[RD1] "Planck alignment plan"
H-P-ASPI-PL-0078 Issue 3 Revision 0. Date of issue: Apr 2004.

[RD2] " Planck Telescope optical analysis"
H-P-3-CSAG-AN-2004 Issue 3 Revision 0. Date of issue: 05/09/2003.

[RD3] "Contamination End of Life needs"
H-P-1-ASPI-TN-0197 Issue 1 Revision 0

[RD4] " Planck Telescope optical budgets"
H-P-3-CSAG-BD-2001 Issue 4 Revision 0. Date of issue: 05/09/2003.

[RD5] "A statistical approach to lens tolerancing"
G. Koch SPIE Vol 147 pp71-82 (1978)

[RD6] Principles of Optics"
Born and Wolf - 7th (expanded) edition

[RD7] "Optical properties of NH_3 ice from the far infrared to the near ultraviolet"
Applied Optics/ Vol. 23 No. 4

[RD8] "Optical constants of ice from the ultraviolet to the microwave"
Applied Optics/ Vol. 23 No. 8

[RD9] "Photochemically deposited contaminants Film Effects"
SPIE Vol 2864 - pp269

[RD10] Cleanliness Meeting #2
H-P-2-ASED-MN-0044 - 05/12/01

[RD11] End of Life cleanliness analysis
H-P-1-ASPI-AN-0269 Issue 3/0

[RD12] Cleanliness Requirements specification
H-P-1-ASPI-SP-0035 Issue 2/1

[RD13] Planck telescope CodeV file
H-P-3-ASPI-TN-0116 issue 2

[RD14] Planck Telescope operational stability budgets
H-P-3-CSAG-BD-2002 issue 2

3. ACRONYMS

HP	**H**erschel-**P**lanck
SRS	**S**ystem **R**equirements **S**pecification
WFE	**W**ave **F**ront **E**rror
OPD	**O**ptical **P**ath **D**ifference
BFE	**B**est **F**it **E**llipsoid
DoF	**D**egree **o**f **F**reedom
LoS	**L**ine **o**f **S**ight
ACMS	**A**ttitude and **C**ontrol **M**onitoring **S**ystem

4. OPTICAL DESIGN DESCRIPTION

The optical model is decribed and detailled in [RD13]

4.1 Planck Telescope

Planck Telescope is an off-axis Gregorian antenna.

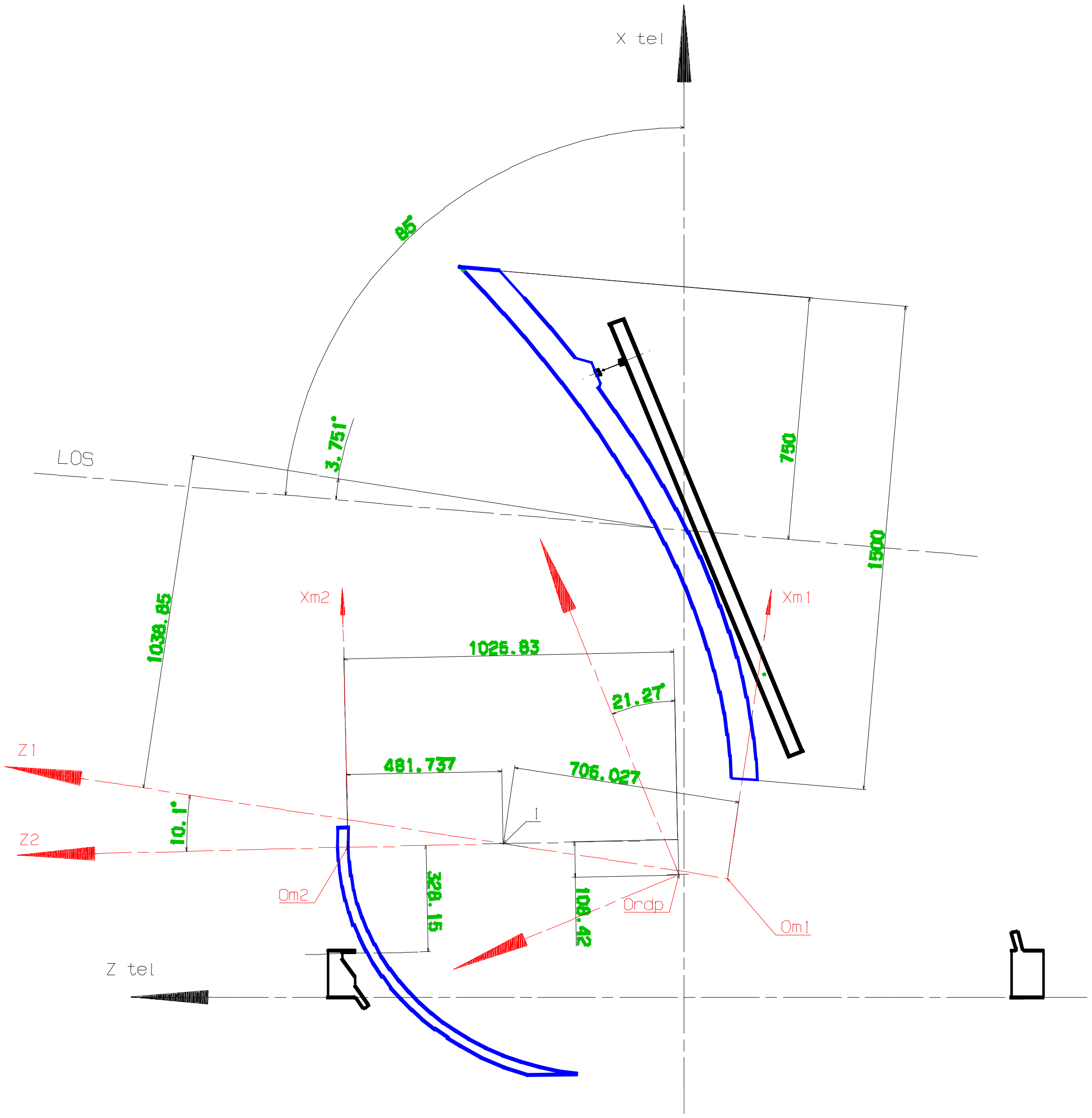

It is composed of two off-axis ellispoids

the optical paraxial characteristics of the are the following:

Aperture	1.5m off-axis
Focal length	1600mm
Field of view	+/-5°
Line of Sight	At 85° of Xtel

This is also shown on the next drawing, with the rays relevant for the center of the field of view

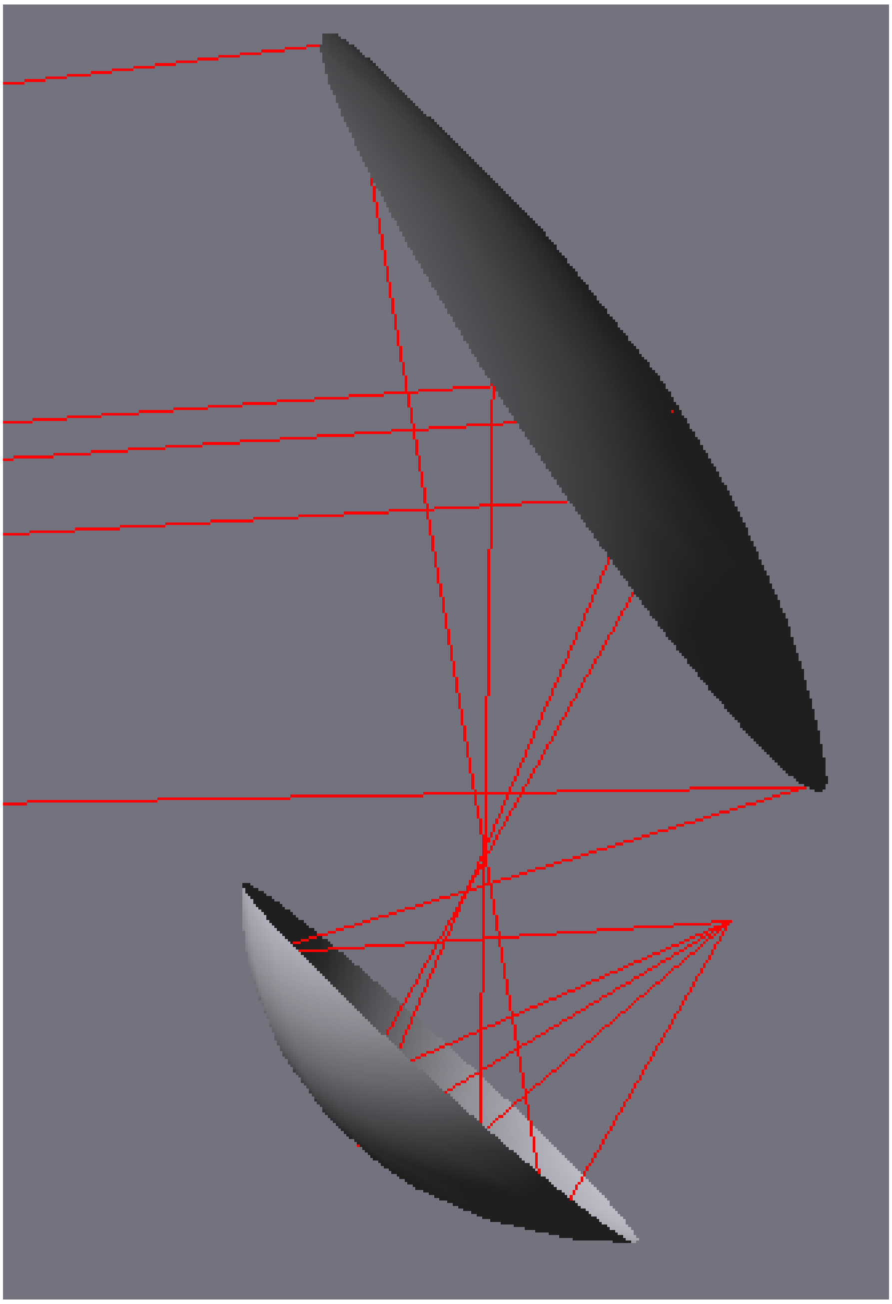

4.2 Focal Plane unit

The focal plane unit is in the hand of ESA and instruments teams. At payload level, it is considered as a single box, and is composed of two instruments, each one is composed of RF detectors, indeed bolometers with horns.
-HFI "High Frequency Instruments" is located at the center of the image field. This is the most sensible to wavefront errors, each HFI horn having its central working wavelength between 0.35mm and 3mm.
-LFI "Low frequency instrument" is located all around HFI, and supports the mechanical interfaces to the payload. This instrument is less sensitive to wavefront errors than HFI, each LFI horn having its central working wavelength between 4.3mm and 10mm.

At each horn corresponds a given central frequency/wavelength, a given position in the field, and a given taper angler (half-cone angle at which the attenuation is -30dB from center)

horns	Taper angle for 30 dB Attenuation (Degree)
L-30-1 to L-30-2	23.6
L-44-1 to L-44-3	23.6
L-70-1 to L-70-6	21.9
H-100-1 to H-100-4	26.8
H-143-1 to H-143-12	23.7
H-217-1 to H-217-12	21.8
H-353-1 to H-353-6	19.4
H-545-1 to H-545-8	19.4
H-857-1 to H-857-6	19.4

This taper angle is optimized with regards to straylight, and particularly spillover, by instruments teams

4.2.1 HFI horns coordinate in RDP coordinate system

	Xrdp	**Yrdp**	**Zrdp**
hfi_100_1	-47,57	-32,966	14,847
hfi_100_2	-55,114	-10,622	16,831
hfi_100_3	-55,114	10,622	16,831
hfi_100_4	-47,57	32,966	14,847
hfi_143_1	33,184	-39,106	-1,28
hfi_143_2	35,142	-16,019	-0,572
hfi_143_3	34,424	16,013	-0,39
hfi_143_4	33,912	41,141	-1,613
hfi_143_5	48,96	-32,843	-4,919
hfi_143_6	50,593	-8,581	-4,455
hfi_143_7	49,882	8,578	-4,263
hfi_143_8	49,672	32,856	-5,108
hfi_217_1	-31,18	-27,749	12,776
hfi_217_2	-29,527	-8,754	13,236
hfi_217_3	-30,307	8,752	13,362
hfi_217_4	-30,399	27,756	12,651
hfi_217_5	-16,174	-34,288	9,791
hfi_217_6	-14,291	-15,164	10,422
hfi_217_7	-15,051	15,16	10,563
hfi_217_8	-15,412	34,298	9,651
hfi_353_1	-3,268	-58,369	5,117
hfi_353_2	-0,512	-39,964	6,325
hfi_353_3	-0,073	-23,141	7,308
hfi_353_4	1,231	-5,905	7,552
hfi_353_5	0,409	10,332	7,649
hfi_353_6	0,451	27,097	6,996
hfi_353_7	-1,536	42,928	6,29
hfi_353_8	-2,513	58,387	4,964
hfi_545_1	12,049	-58,768	1,867
hfi_545_2	14,698	-40,242	3,022
hfi_545_3	13,702	43,225	3,004
hfi_545_4	12,784	58,788	1,703
hfi_857_1	15,072	-23,799	3,974
hfi_857_2	16,357	-6,442	4,207
hfi_857_3	15,568	9,909	4,332
hfi_857_4	15,617	27,287	3,672

Since SRR, the location of the HFI horns have been updated according to [RD6]

4.2.2 LFI horns in RDP coordinate system

	X	Y	Z
LFI_70_18	-76,38	-69,37	14,54
LFI_70_19	-92,41	-43,29	18,66
LFI_70_20	-101,86	-17,69	20,86
LFI_70_21	-101,86	17,69	20,86
LFI_70_22	-92,41	43,29	18,66
LFI_70_23	-76,38	69,37	14,54
LFI_44_24	-138,41	0	21,29
LFI_44_25	55,32	133,27	-17,9
LFI_44_26	55,32	-133,27	-17,9
LFI_30_27	-136,95	54,94	18,6
LFI_30_28	-136,95	-54,94	18,6

4.3 reflectors

The Planck reflectors are a Customer furnished Equipement, specified ain [AD2].

As the telescope is basically an optimized of-axis gregorain telescope, the PR is almost a parabola, and the SR is an ellipsoid.
The characteristics of the optical surfaces are the following:

PERF-005 *The ellipsoid surface profile defined in the optical reference frames at operating conditions and in dry conditions shall be:*

$$z = \frac{p/r}{1+\sqrt{1-(K+1)\frac{p}{r^2}}} \qquad p = x^2 + y^2$$

with x, y and z the coordinates in the mirror axis systems

With the following parameters:

Parameters	**PR**	**SR**
Radius of curvature of the ellipsoid: r (mm)	1440.000	- 643.972
Conic constant : K	- 0.86940	- 0.215424

As decribed in [AD5] the deltas with regards to the theoretical surfaces (either computed by FEM or measured) are considered in the optical analyses

5. WAVE-FRONT ERROR

5.1 Definition

The optical quality of the Planck Telescope is specified in terms of Wave Front Error. This is a classical way to specify the ability of a optical imaging system to perform a sharp image. The Wave Front is the surface of equal phase (iso-OPD) produced by a point source. The entrance Wave-Front, coming from cold space, is flat. If the telescope is perfect (i.e. free of aberration) the output wavefront is a sphere, centered on the focal point - this is linked to the fact that all the light "rays" of geometrical optics converge on a single focal point. It gives a perfect "diffraction-limited" image point. However, the actual telescope will not be perfect, because of reflectors distortions and misalignments of the reflectors and FPU, and the Wave Front is thus distorted.

For a given ray, the OPD (for Optical Path Difference) is the normal deviation of the actual phase from the theoretical one. By hypothesis, the chief ray is considered as a reference, and it's OPD is set to zero. The Root-mean-square value of these differences over the pupil, for a given entrance field angle, is the WFE rms. This can be expressed in wavelength for monochromatic systems. For Planck, due to the large spectral domain covered by the several detectors, it will be expressed in micrometers.

The previous considerations are valid when the following classical hypotheses are made:

- The reference is the perfect optical system (for which WFErms = 0µm)
- The intensity distribution is constant over the pupil

For Planck, the previous hypotheses are not verified because, on one hand, the theoretical WFE is not completely negligible, and on the other hand, the RF detector taper induces a pupil amplitude apodisation, which has to be taken into account in the WFE computation. These two particular points will be further explained in the next sections.

5.1.1.1 Impact of non perfect theoretical optical design.

In the frame of Planck Architect Study, the optical design of the telescope has been optimized - via optical design software CodeV- in order to have a correct image quality over the field of view, taking into account the fact that the more the detectors are in the field, the higher their working wavelength is. It led to have a better theoretical wavefront in the center than in the field.

The following graph also illustrates this point. It gives the theoretical Wave Front Error in microns for some typical horns:

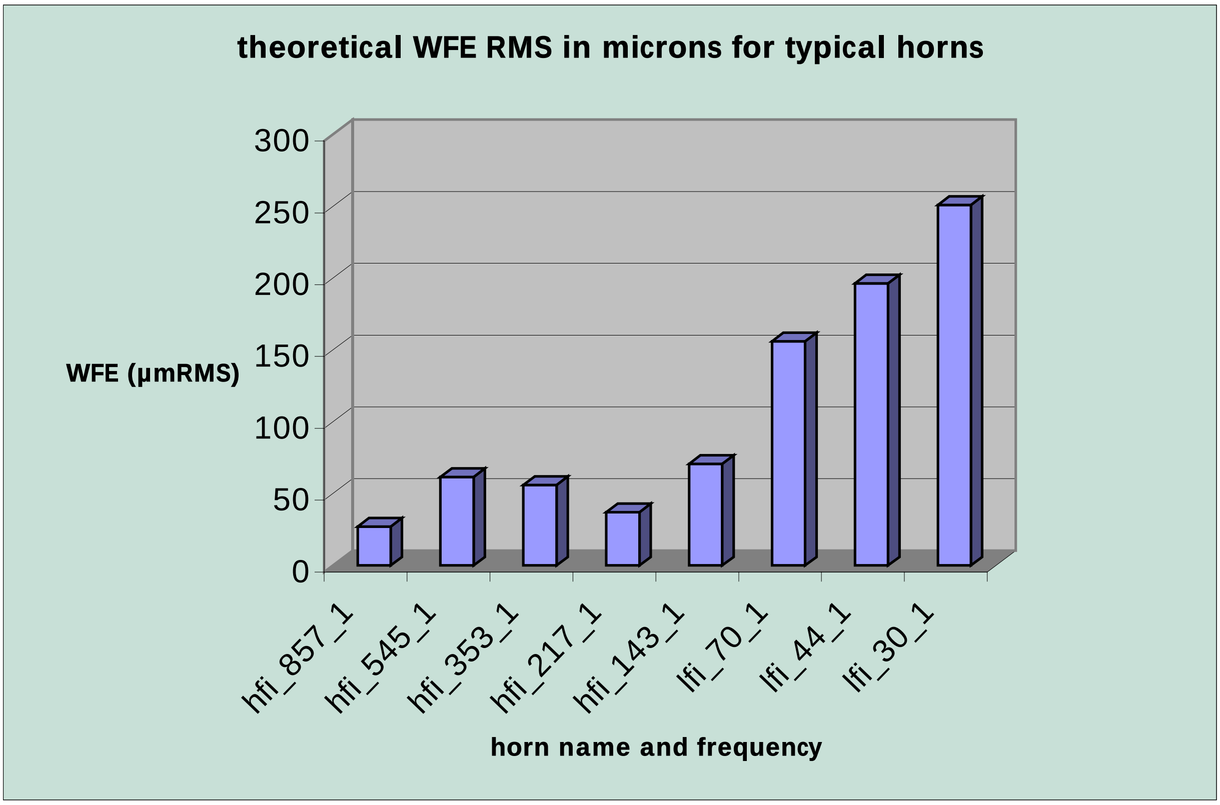

To analyze the impact of the perturbation on the optical quality, one have to be able to assess the impact of a small perturbation on a non-perfect wave-front. In that context, the simple usual ways to compute WFE, subtracting (RMS or linear) the theoretical WFE from the actual is not accurate. The proper way to assess the impact of a perturbation on a such a non-perfect system is to subtract Wavefronts (i.e a two dimension curve) and to compute the RMS value of this "Wavefront Differential".

5.1.1.2 Impact of apodization

In classical optical systems, the entrance pupil is uniformly irradiated, and the detector response do not depend significantly on the ray incidence. However, Planck detectors are RF horns, which are "tappered". This means that they are less sensible to rays coming from the edge of the pupil than to rays coming from the center, This pupil attenuation is also called apodization (This is linked to the fact that a smooth variation of the intensity from the center to the edge of the pupil tends to attenuation the far side lobes i.e. the "feet" of the PSF)

In the frame of the optical analysis, the apodization will be considered as a gaussian function (as specified in [AD1]). The exact apodization is not exactly gaussian, and is taken into account in RF analyses.

For example, gaussian apodization of -20dB from the center to the edge gives the following amplitude repartition - linear and log graphs:

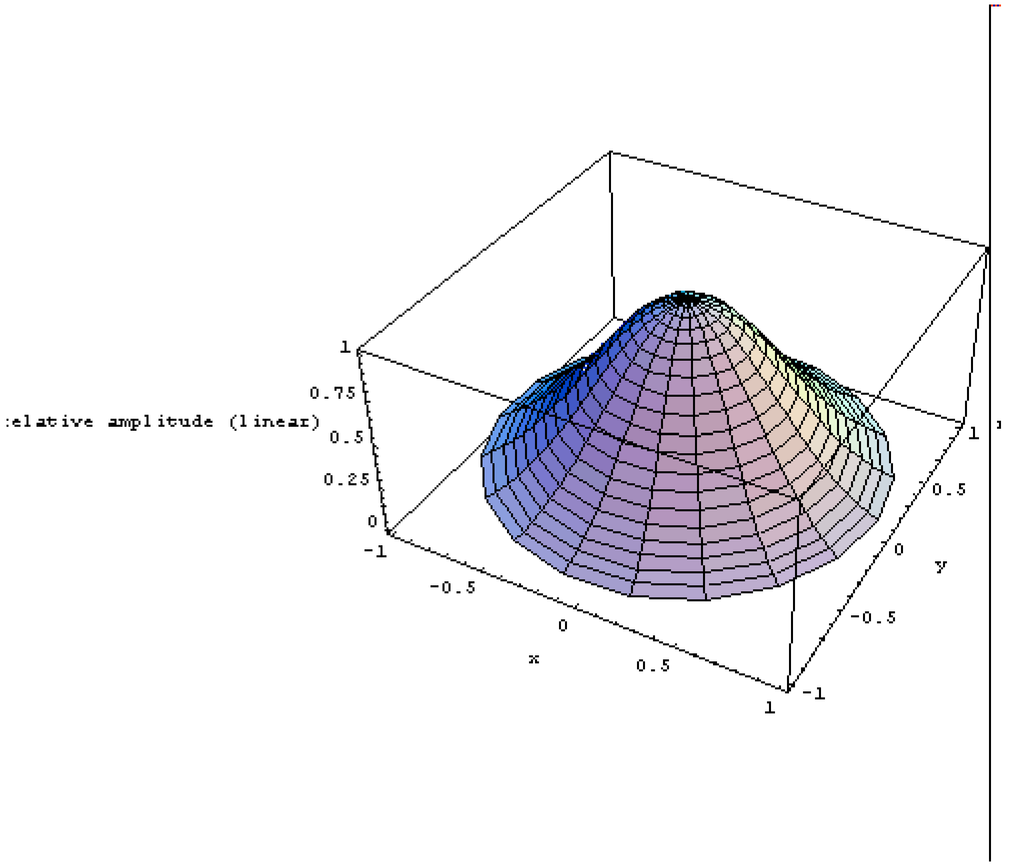
elative amplitude (linear)
1
0.75
0.5
0.25
0
-1
-0.5
0
0.5
1
x
-1
-0.5
0
0.5
1
y

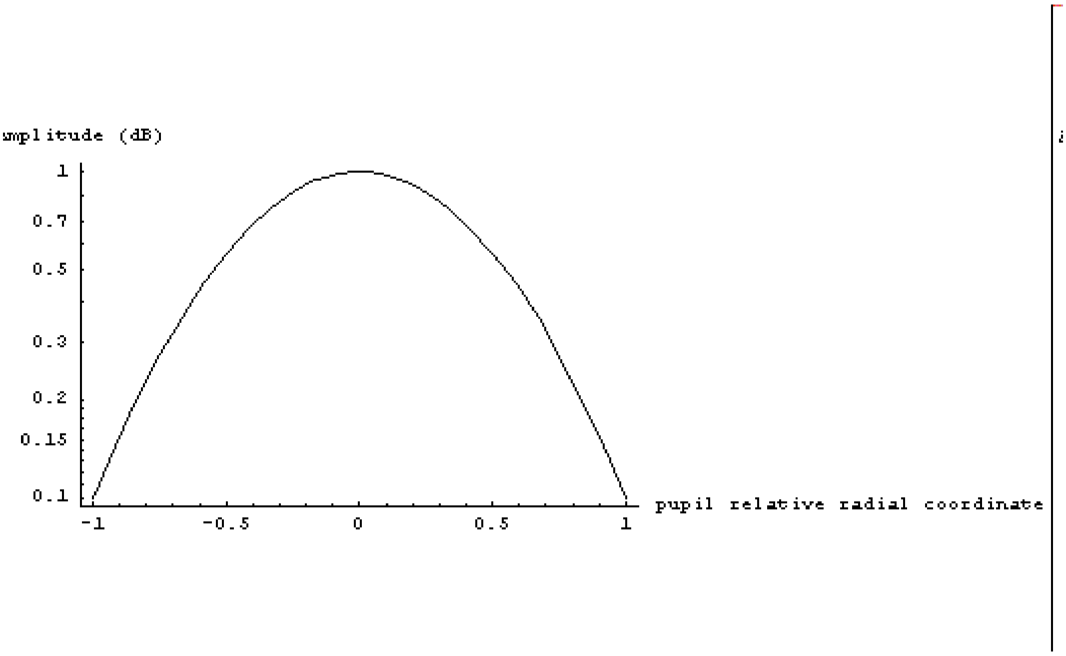
mplitude (dB)
1
0.7
0.5
0.3
0.2
0.15
0.1
-1
-0.5
0
0.5
1
pupil relative radial coordinate

The following table recalls the taper angle and the relevant attenuation for the several Planck Horns:

horns	**Taper angle for 30 dB Attenuation (Degree)**
L-30-1 to L-30-2	23.6
L-44-1 to L-44-3	23.6
L-70-1 to L-70-6	21.9
H-100-1 to H-100-4	26.8
H-143-1 to H-143-12	23.7
H-217-1 to H-217-12	21.8
H-353-1 to H-353-6	19.4
H-545-1 to H-545-8	19.4
H-857-1 to H-857-6	19.4

These apodizations have to be considered on horn side. In the "object space", the projected apodization is not exactly gaussian, because of pupil aberrations.

This apodization has an impact on how to compute WFE. It has to be taken into account, because the OPD of rays coming from the edge of the pupil, are less seen than the one coming from the center of the pupil. The apodization can be considered as an amplitude transmission variation T from the center to the edge of the pupil. The following formula shows how this transmission variation has to be taken into account in WFE assessment, for a given field:

$$\left[\frac{WFE}{\lambda}\right]^2 = \frac{\iint_{pupil\ surface} T\Delta^2 d^2S}{\iint_{pupil\ surface} Td^2S} - \left[\frac{\iint_{pupil\ surface} T\Delta d^2S}{\iint_{pupil\ surface} Td^2S}\right]^2$$

Equation 1 Apodized Wavefront error- analytical formula

where Δ is the OPD on a given ray

This formula has been extracted from a classical book ("Diffraction - structure des images" A. Maréchal & M. Françon 1970), and cross-validated with CodeV . This cross-validation is presented in the next section

5.2 Requirement

The requirement, as expressed in Planck Telescope Design Spec (cf. [AD1]), is the following:

"

The required telescope performance is defined w.r.t. the theoretical performance

TPE-030 The telescope shall achieve a WFE at the defined position of the detectors and operational conditions that does not degrade the theoretical value by more than see table:

Instrument	Frequency	Default max contribution	
	GHz	Goal micron RMS	Specs. micron RMS
LFI	30	80	119
	44	61	92
	70	61	92
HFI	100	48	72
	143	40	60
	217	38	57
	353	33	50
	545	32	48
	857	28	42

Note: The final WFE = $\sqrt{(\text{max theoretic WFE})^2 + (\text{default max contribution})^2}$

"

5.3 WFE computation.

The wave-front error might either be computed "by hand", as it was doneto assess the reflectors performance due to MSSE, or by simulating on the optical software CodeV. The "Apodized WFE" as defined in the preceding section is not usual in optics. So, the formula and CodeV were cross-checked on that point. It was done by computing some simple errors, such as defocus, by hand, and by checking the results done by CodeV. This is presented in this section.

In this section, we will consider the impact of a given error on a perfect (flat) mirror. The error is firstly defined in terms of Zernike polynomials. It is then calculated "by hand" using the theoretical formula, and finally the result given by CodeV for the same case is presented.

In these examples, the working wavelength is 1µm.

5.3.1.1 Example 1: Perfect imaging:

In this case, $\Delta=0$ all over the pupil, and thus WFE=0 µm. This is also the result given by CodeV
->good correlation

5.3.1.2 Example 2: Defocus

In the case where the error on a mirror is simply defocus. It is simulated by the Zernike polynomial Z_4:

$$Z_4(r,\theta)=2r^2-1$$

Equation 5-2

Let's consider a 1µm mechanical error at the edge of the flat pupil. We then have:

$$MSSE(r,\theta)=1*(2r^2-1)$$

Equation 5-3

5.3.1.2.1 non apodised case

5.3.1.2.1.1 analytical calculation:

Taking into account that :

$\Delta=2*\cos(\alpha_i)*MSSE(r,\theta)=2*(2r^2-1)$

$T(r,\theta)=1$ (no apodization) ,

Equation 1 becomes:

$$\left[\frac{WFE}{\lambda}\right]^2=4*1*\left[\frac{\iint_{pupil}(2r^2-1)^2d^2S}{\iint_{pupil}d^2S}-\left[\frac{\iint_{pupil}(2r^2-1)d^2S}{\iint_{pupil}d^2S}\right]^2\right]$$

Equation 5-4

$$\iint_{pupil}(2r^2-1)^2 d^2S = \int_0^{2\pi}\int_0^1 (2r^2-1)^2 \frac{1}{\pi} r dr d\theta = \frac{1}{3}$$

$$\iint_{pupil} d^2S = 1$$

$$\iint_{pupil}(2r^2-1)\ d^2S = \int_0^{2\pi}\int_0^1 (2r^2-1)\frac{1}{\pi} r dr d\theta = 0$$

which leads to $\left[\frac{WFE}{\lambda}\right]^2 = 4*1*\left[\frac{1/3}{1}-0\right] = 1/75 = 1.333$

$$\frac{WFE}{\lambda} = 1.155$$

5.3.1.2.1.2 CodeV

CodeV leads to $\frac{WFE}{\lambda} = 1.151$

->good correlation

5.3.1.2.2 apodised case

Let's here consider a gaussian apodisation of -20dB at the edge of the pupil.

The amplitude T over the pupil is then defined by $\frac{T(r,\theta)}{T_0} = e^{-\left(\frac{r}{a}\right)^2}$, where a is chosen to lead to $20\log\left(\frac{T(1,\theta)}{T_0}\right) = 20\log\left(e^{-\left(\frac{1}{a}\right)^2}\right) = -20$ dB amplitude at the edge of the reflector pupil:

The proper value of a is 0.659, and we then have:

$\frac{T(r,\theta)}{T_0} = e^{-\left(\frac{r}{0.659}\right)^2}$ i.e. $\frac{T(1,\theta)}{T_0} = 0.1$ amplitude at the edge.

5.3.1.2.2.1 analytical calculation:

Taking into account that :

$$\Delta = 2*\cos(\alpha_i)*MSSE(r,\theta) = 2*(2r^2-1)$$

$$\frac{T(r,\theta)}{T_0} = e^{-\left(\frac{r}{0.659}\right)^2}$$

Equation 1 becomes:

$$\left[\frac{WFE}{\lambda}\right]^2 = 4*1*\left[\frac{\iint_{pupil} e^{-\left(\frac{r}{0.659}\right)^2}(2r^2-1)^2\,d^2S}{\iint_{pupil} e^{-\left(\frac{r}{0.659}\right)^2}\,d^2S} - \left[\frac{\iint_{pupil} e^{-\left(\frac{r}{0.659}\right)^2}(2r^2-1)\,d^2S}{\iint_{pupil} e^{-\left(\frac{r}{0.659}\right)^2}\,d^2S}\right]^2\right]$$

Equation 5-5

$$\iint_{pupil} e^{-\left(\frac{r}{0.659}\right)^2}(2r^2-1)^2\,d^2S = \int_0^{2\pi}\int_0^1 e^{-\left(\frac{r}{0.659}\right)^2}(2r^2-1)^2\,\frac{1}{\pi}\,r\,dr\,d\theta = 0.151$$

$$\iint_{pupil} e^{-\left(\frac{r}{0.659}\right)^2}\,d^2S = 0.391$$

$$\iint_{pupil} e^{-\left(\frac{r}{0.659}\right)^2}(2r^2-1)\;d^2S = \int_0^{2\pi}\int_0^1 e^{-\left(\frac{r}{0.659}\right)^2}(2r^2-1)\,\frac{1}{\pi}\,r\,dr\,d\theta = -0.138$$

which leads to $\left[\frac{WFE}{\lambda}\right]^2 = 4*1*\left[\frac{0.151}{0.391} - \left[\frac{-0.138}{0.391}\right]^2\right] = 1.046$

thus, $\frac{WFE}{\lambda} = 1.0230$

5.3.1.2.2.2 CodeV

CodeV leads to $\frac{WFE}{\lambda} = 1.0235$
->again good correlation

5.3.1.3 Example 3: Pure spherical aberration

The case of Pure spherical aberration has also be treated. A good accordance between the formula and CodeV (cf. results in the conclusion hereafter)

5.3.1.4 Conclusion:

The comparison of the results coming from the formula and from CodeV is presented in the table hereafter:

Wfe/λ	Without apodization		With 20dB apodization	
	Formula	CodeV	Formula	CodeV
Perfect system	0	0	0	0
1µm defocus	1.155	1.151	1.023	1.023
1µm spherical aberration	0.8944	0.8958	0.941	0.933

The results are quasi-identical. The differences are always below 1%
The formula (cf. Equation 1), and the way CodeV computes WFE (with and without apodisation) are validated.

5.4 sensitivities

In this section, we will focus on the sensitivity FPU position. The sensitivity to reflectors decenters and tilts have been preliminary presented by Alcatel in the frame of the SRR, and are currently managed by Contraves. They are a part of Contraves PDR data package.

The sensitivity of FPU position to WFE has been assessed via CodeV optical analysis software. The results are presented in the following sections, where the WFE in µm is presented, as a function of FPU displacement, along Z (focus), X, and Y (in the field).

Note: the optical model has been updated since the PDR - see [RD13] ; the rays were not completely filling PR at that time). This increases slightly the sensitivities.

5.4.1 Sensitivity to defocus

In the preceding graph, the WFE variation, computed as explained in section 5.3, is presented as a function of a global FPU defocus. For a classical optical system, all the field points (detectors) would have the same sensitivity. However, on Planck, a detector has an dedicated apodization, which makes it more or less sensible to rays coming from the edge of the pupil, and thus more or less sensitive to aberrations. This explains why HFI horns at 857GHz, 545 GHz and 353GHz have the same sensitivity: they have indeed the same apodization.

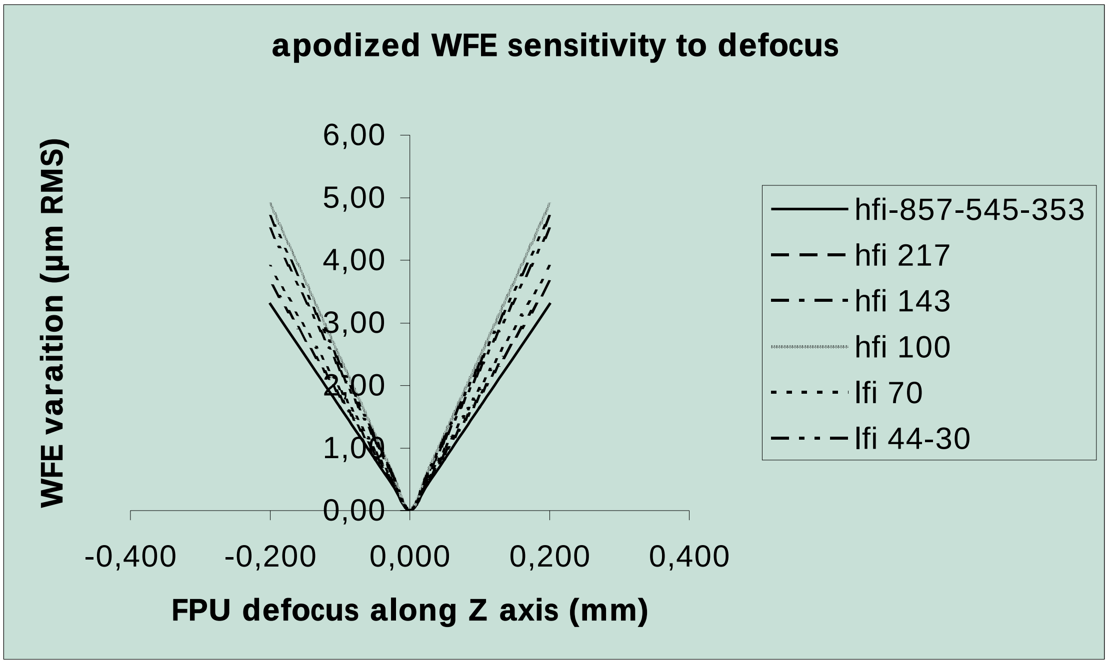

As a conclusion, the preceding graph shows that the more sensitive horns are the hfi 100GHz with 2.3µm WFE variation /0.1mm defocus, whereas the less sensitive horns are the high frequency hfi, with 1.27µm WFE variation /0.1mm defocus.

5.4.2 Sensitivity to FPU radial displacement

As the focal surface is not included in a plane, the lateral displacement (perpendicular to defocus Z_{RDP}), induces a defocus, which depends of the curvature of the focal surface at the horn position. In the following graph, we present the sensitivity along X_{RDP} (in the telescope symetry plane) and along Y_{RDP}.

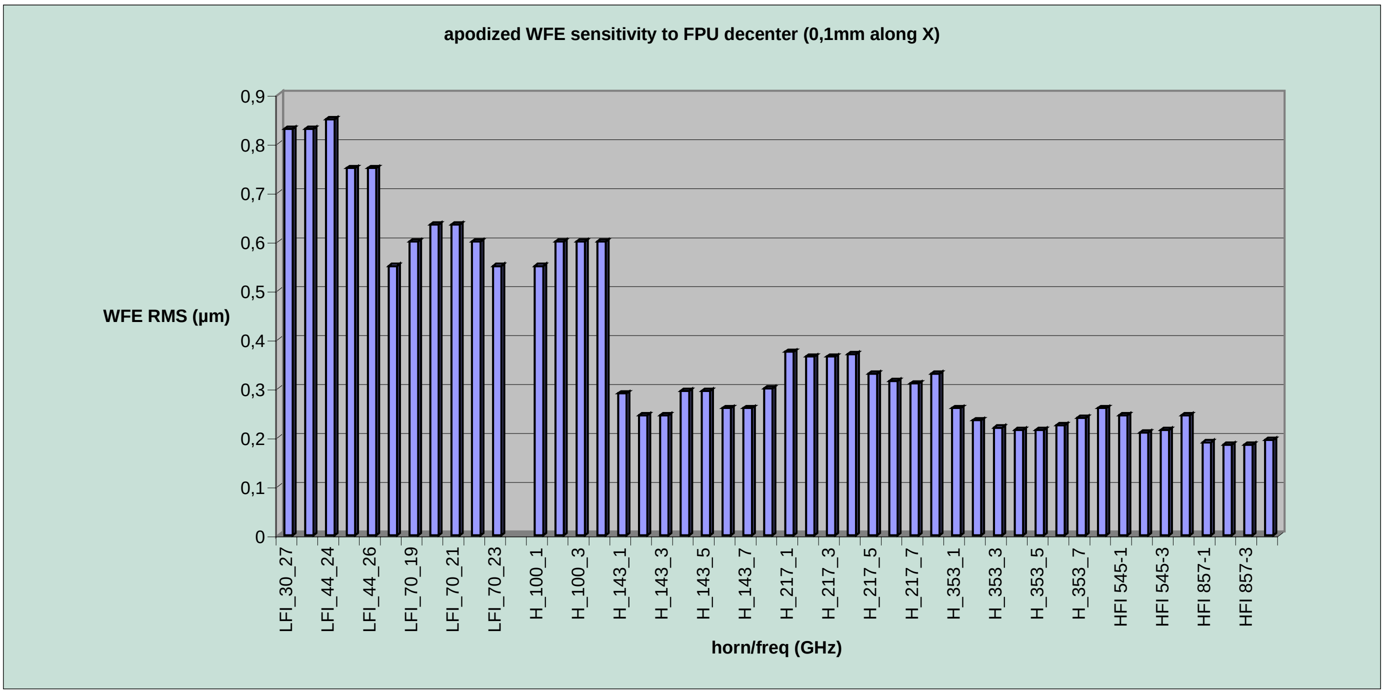

Depending on their location and apodization, horns might be more or less sensitive to FPU X displacment. Sensitivity is include between 0.8µm WFE RMS/0.1mm for 30GHz LFI horns and 0.15µm WFE RMS/0.1mm for 857GHz HFI horns

The same analysis for a displacement along Y (perpendicular to telescope symmetry plan), leads to the following sensitivity:

Again, depending on their location and apodization, horns might be more or less sensitive to FPU Y displacement. Sensitivity is included between 0.8µm WFE RMS/0.1mm for 30GHz LFI horns and 0.05µm WFE RMS/0.1mm for some 857GHz and 353 HFI horns

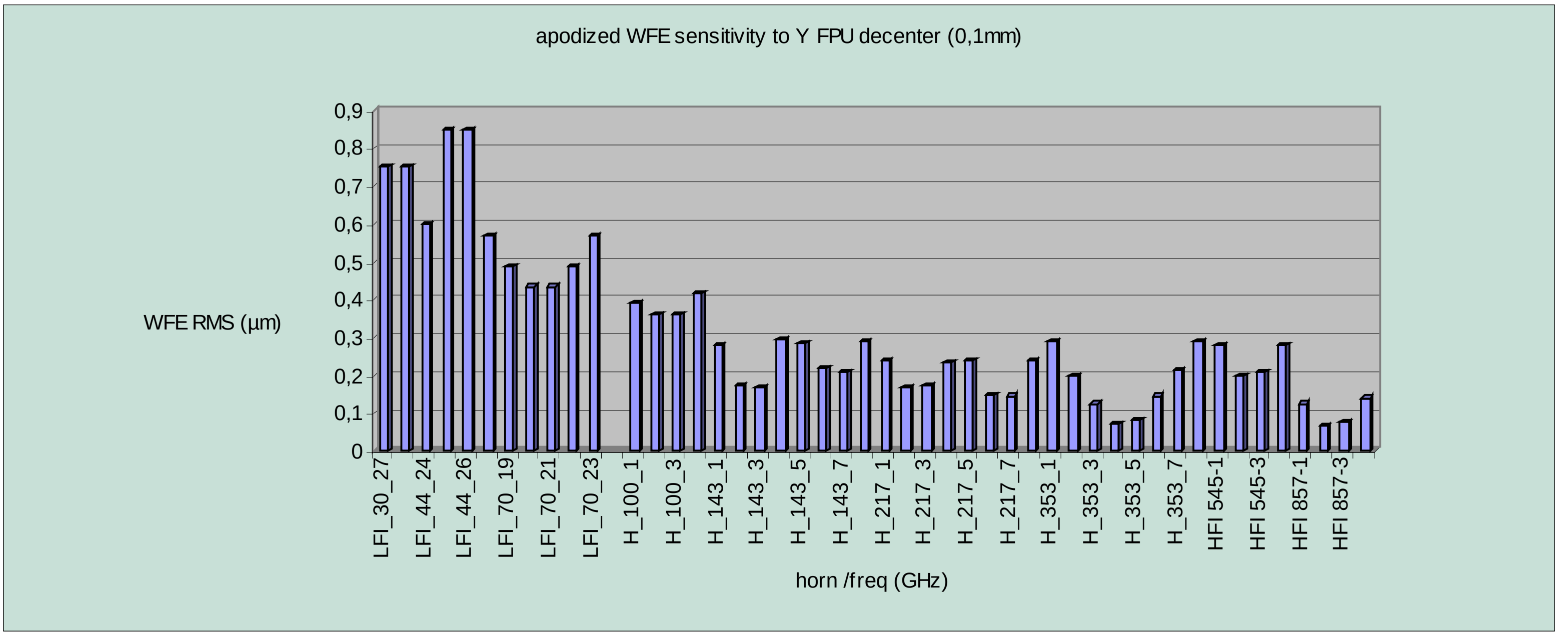

5.5 WFE Performance analysis

The contributors tree is the following:

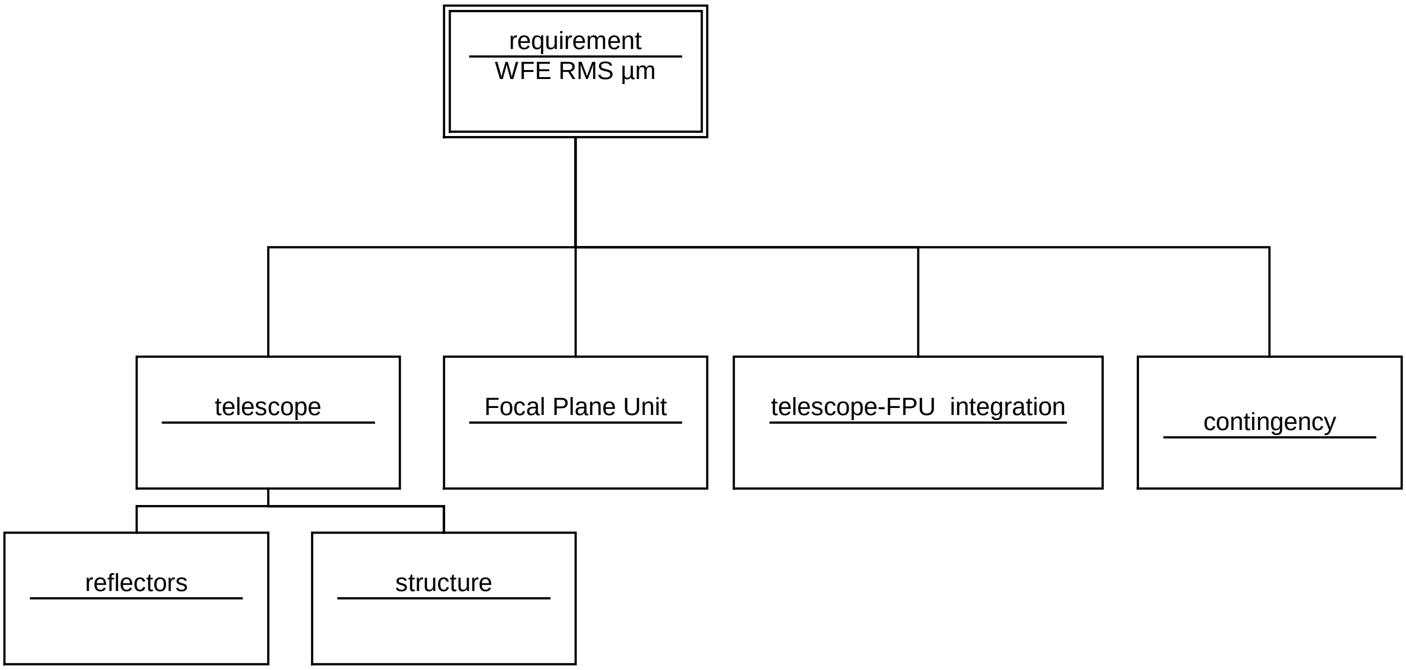

5.5.1 Budget architecture and summation rule

The budgets traets separately the deterministic load cases and the random one. See [RD5] for a more extensive justification and description of this approach.

5.5.1.1 Deterministic load case

The deterministic load case is the sum in terms of displacements and reflectors distorsions of all the signed individual load cases. This represents our best estimate (most probabale) telescope configuration in-orbit.
The deterministic load case covers:

- cool-down
- gravity release
- moisture release
- reflectors manufacturing (the QM reflectors shape are considered)

This is entered, as a single load case in the optical model, and after substraction of the theoretical wavefront, one apodized WFE per horn is computed

This load case is described in [AD5]

5.5.1.2 Random load cases

On top of the deterministic, a lot of uncertainties do exist at this stage, each one possibly degrading (or improving) the optical performance.
They cover

- Manufacturing accuracy
- Measurement accuracy (incl. Material properties)
- Alignment accuracy
- Modeling accuracies

The impact in terms of apodized WFE of each one of them is computed individually for each horn at 2 sigma probability level. Based on the hypotheses that the random load cases are

  - Non correlated
  - Independant
  - On the same order of magnitude

The central theorem applies, which enables us to compute the final 2sigma probability level degradation by simply summing RSS the single 2 sigmas WFE degradation

5.5.1.3 Summation rule

Deterministic load case contribution and random contribution are summed linearly

5.5.1.4 Schematic description

The following graph represent the final WFE distribution law

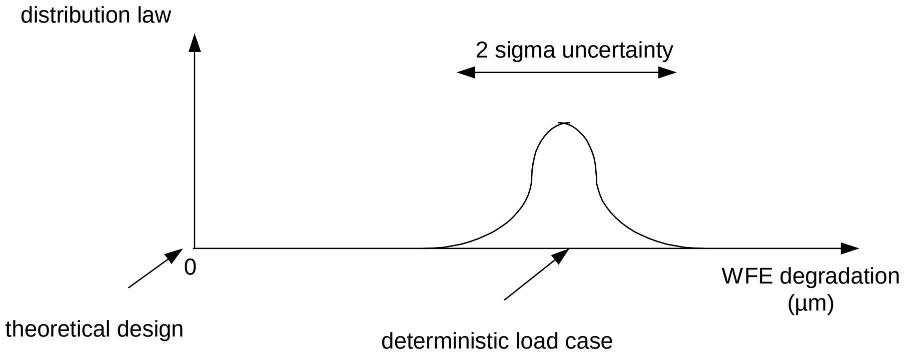

5.5.2 Contributors analyses

The following contributors have to be considered in the eterministic case:

- Moisture release
- High Spatial Frequency reflectors shape defects (as measured on QM reflectors)
- In-orbit gradients
- Deterministic mechanical IF displacements
- Dimpling
- Gravity

5.5.2.1 Deterministic load case

The ideal wavefront (without any load case), for the center of the field of view, is the following:

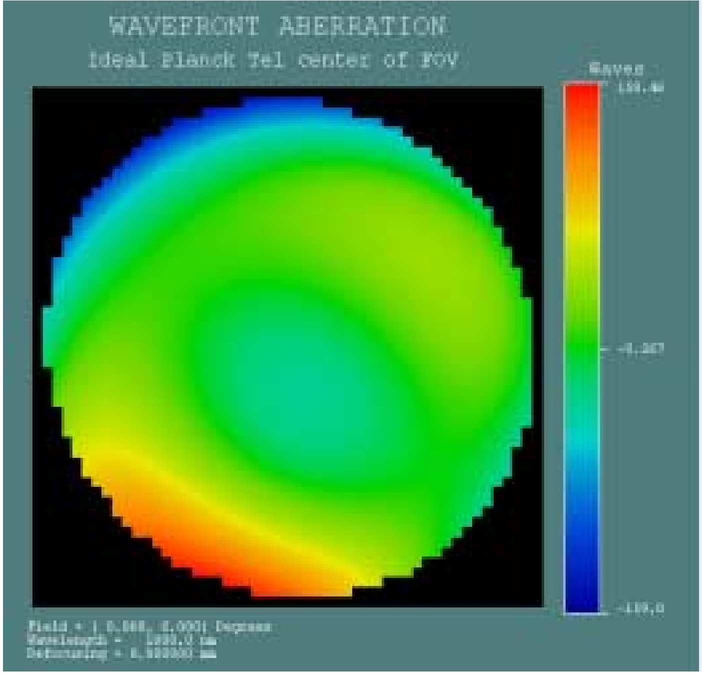

note that this is a phase map, and that the amplitude apodization is thus not represented here.

The deterministic load case is described in [AD5] gives the following wavefront degradation at the center of the field:

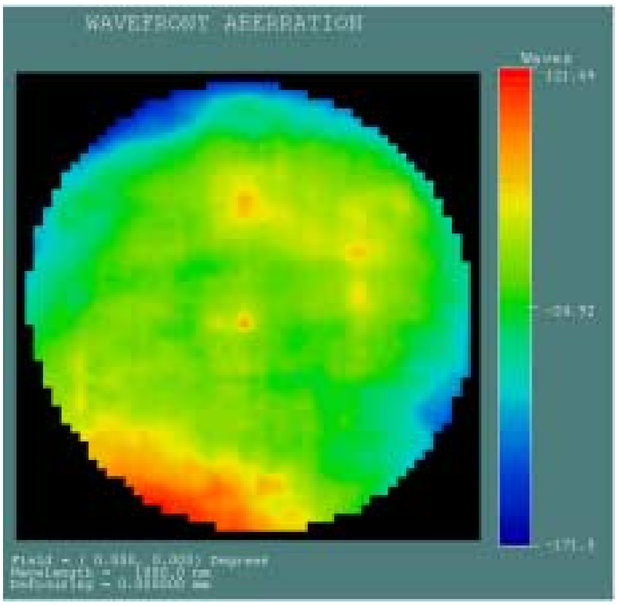

The general wavefront shape remains (and so does the PTV value), the main obvious difference being the high frequency errors, coming from the reflectors manufacturing
To better identify the impact of the deterministic load case, the theoretical wavefront is substracted fom the actual one, giving the following wavefront degradation:

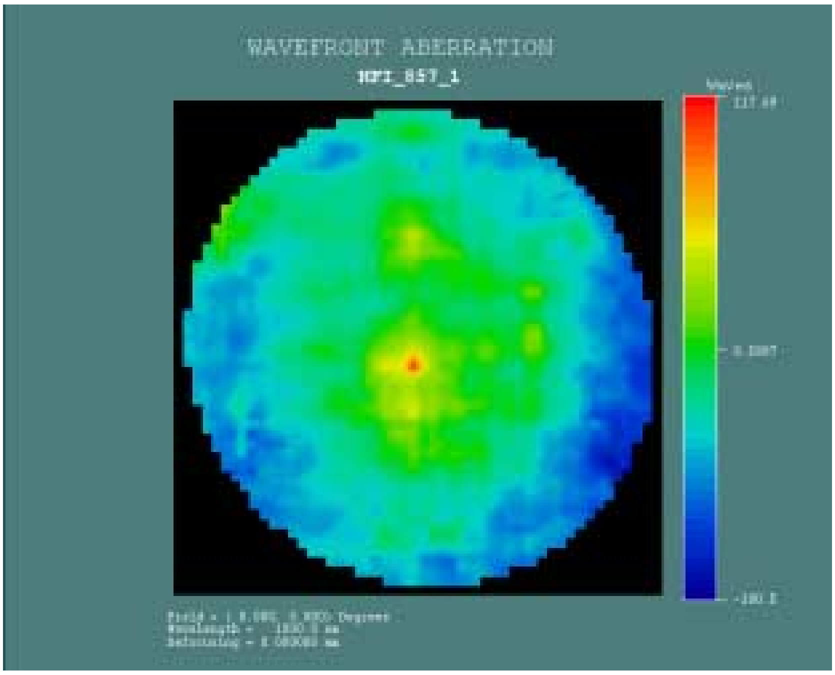

The high frequency distorsions are clearer, and we see also low frequency distorsions: a combination of defocus, astigmatism and coma. The followinf figure is a 3D map of the wavefront degradation (arbitrary units and axis names):

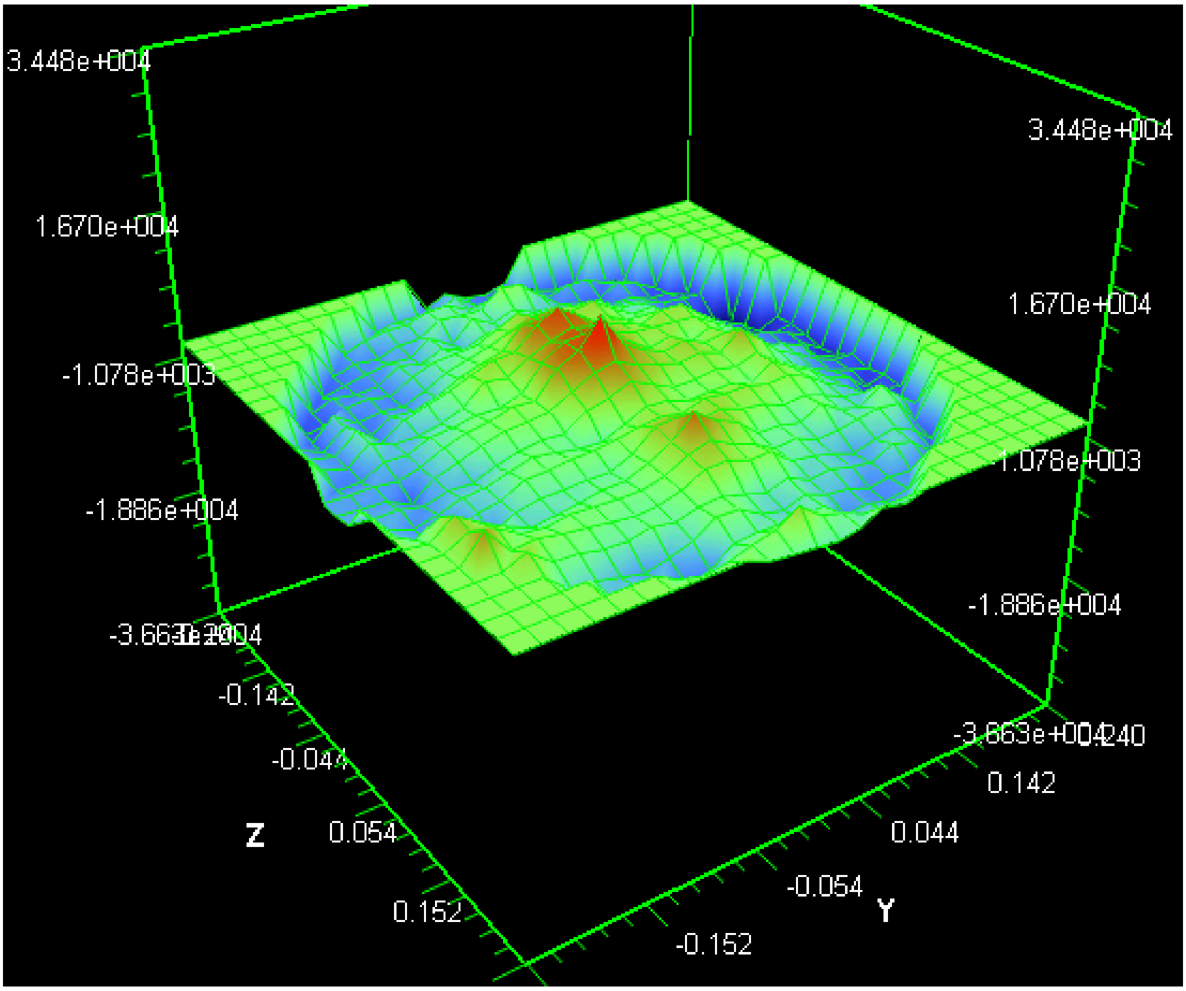
3.448e+004
1.670e+004
-1.078e+003
-1.886e+004
-3.663e+004
3.448e+004
1.670e+004
1.078e+003
-1.886e+004
-3.663e+004
0.240
-0.142
-0.044
Z
0.054
0.152
0.142
0.044
-0.054
Y
-0.152

Once apodized, at the center of the field of view, the deterministic wavefront degradation is 22.7µm RMS.

The operation is made for all the horns, and lead to the following table:

	Deterministic Apodized WFE (µm)
hfi_100_1	22,9
hfi_100_2	25,5
hfi_100_3	24,4
hfi_100_4	24,1
hfi_143_1	24,7
hfi_143_2	24,8
hfi_143_3	24,6
hfi_143_4	24,1
hfi_143_5	24,4
hfi_143_6	25,4
hfi_143_7	24,4
hfi_143_8	23,9
hfi_217_1	23,5
hfi_217_2	23,2
hfi_217_3	23,0
hfi_217_4	22,5
hfi_217_5	23,8
hfi_217_6	23,2
hfi_217_7	22,0
hfi_217_8	22,4
hfi_353_1	22,6
hfi_353_2	22,3
hfi_353_3	21,7
hfi_353_4	22,0
hfi_353_5	21,5
hfi_353_6	20,9
hfi_353_7	21,2
hfi_353_8	21,0
hfi_545_1	22,0
hfi_545_2	21,7
hfi_545_3	21,3
hfi_545_4	20,9
hfi_857_1	22,7
hfi_857_2	22,7
hfi_857_3	22,7
hfi_857_4	22,7

	Deterministic Apodized WFE (µm)
LFI_30_27	21,88
LFI_30_28	24,31
LFI_44_24	22,60
LFI_44_25	25,12
LFI_44_26	29,19
LFI_70_18	24,92
LFI_70_19	24,71
LFI_70_20	24,71
LFI_70_21	23,44
LFI_70_22	22,83
LFI_70_23	21,12

This is represented on the next graph

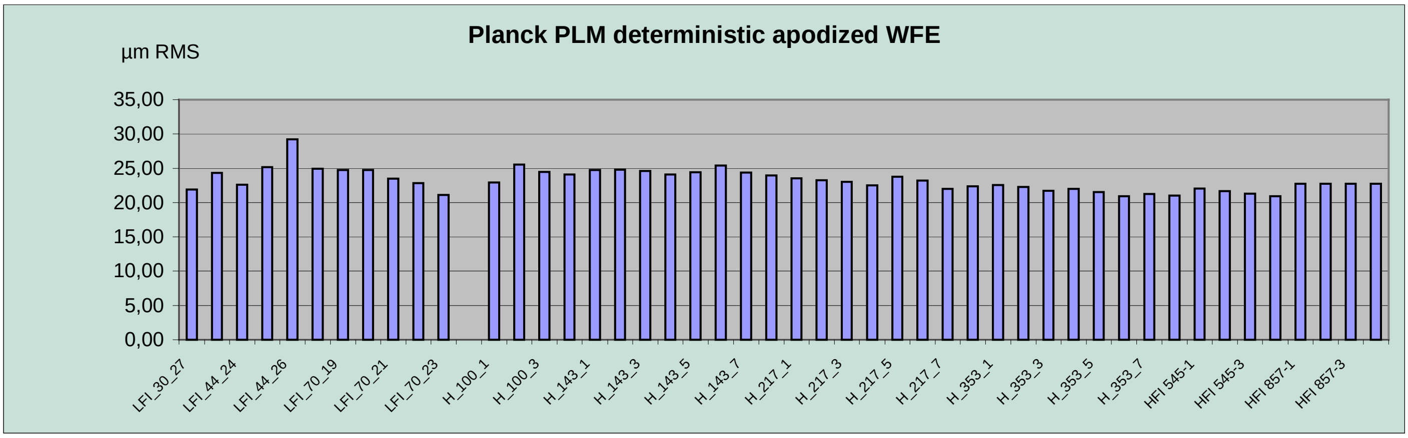

5.5.2.2 Random load cases

The random load cases are described in [AD5]. They are recalled hereafter

			Tx	**Ty**	**Tz**	**Rx**	**Ry**	**dR**	**dK**	**Refocus? (**)**	**Correlated? (***)**
			µm	µm	µm	µrad	µrad	µm			
PR	QM Videogram.		60	0	60	0	108	0	0	Yes	No
	QM T scaling		-12	0	-3.4	0	0.2	0	0	Yes	Yes(*)
	QM T know		-2.5	0	-0.7	0	0.0	0	0	Yes	Yes(*)
	CTE non-unif	Frame	4.4	0.1	-2.6	0	-2.3	0	0	Yes	Yes(*)
		Pr pan	-17.5	0	-4.3	0	-29.4	0	0	Yes	Yes(*)
		SR pan	-0.2	0	-0.2	0	-0.3	0	0	Yes	Yes(*)
		Fr st1	-0.6	0.8	-8.7	-6.9	0.8	0	0	Yes	Yes(*)
		Fr st2	-0.6	-0.8	-8.6	9	0.8	0	0	Yes	Yes(*)
		BBS	-0.4	0	9.6	0	-25.7	0	0	Yes	Yes(*)
		BTS	-0.4	0	8.6	0	-23.2	0	0	Yes	Yes(*)
		Sr st1	0	0.1	0	-0.1	0	0	0	Yes	Yes(*)
		SR st2	0	-0.1	0	0.1	0	0	0	Yes	Yes(*)
		Low st	-0.5	0	0	0	-1.2	0	0	Yes	Yes(*)
	CS IF load		3.3	-0.5	-1.13	0.2	8.6	0	0	No	No
	Baffle IF load		4.5	0.0	12	-0.1	-2.3	0	0	Yes	No
	FPU IF load		3.9	0.0	-0.85	0.0	11.5	0	0	No	No
	PR, SR, JFET		-1.83	0.0	0	0.0	-3.2	0	0	Yes	No
	Gravity release		5.7	0.0	-11.5	0.0	20.0	0	0	No	No
	Moist release	Struc	-4.6	0.0	2.1	0.0	-9.3	0	0	No	No
		refl	-12	0	1.37	0	12.3	-13.2	2.7 10-5	No	Yes
	Alignment		152	152	152	22.4	22.4	0	0	Yes	No
	CS planarity	E	-0.6	0	-37.2	0	92.6	0	0	No	Yes(*)
		N-E	-31.7	53.6	1.6	-21.7	-48.2	0	0	No	Yes(*)
		N-W	4.2	-8.5	47.4	50.3	-4.1	0	0	No	Yes(*)
		W	0.4	0	-0.8	0	1.4	0	0	No	Yes(*)
		S-W	4.2	8.5	47.4	-50.3	-4.1	0	0	No	Yes(*)
		S-E	-31.7	-53.6	1.6	21.7	-48.2	0	0	No	Yes(*)
	TTA	E	-1.1	0	-8.07	0	18.7	0	0	No	Yes(*)
		N-E	-6.34	10.82	-0.17	-4.0	-7.8	0	0	No	Yes(*)
		N-W	0.28	-0.42	7.8	7.5	-1.7	0	0	No	Yes(*)
		W	0.1	0	0.22	0	0.2	0	0	No	Yes(*)
		S-W	0.28	0.42	7.8	-7.5	-1.7	0	0	No	Yes(*)
		S-E	-6.34	-10.8	-0.2	4.0	-7.8	0	0	No	Yes(*)
	Structure launch		20	20	20	20	20	0	0	No	No
	Structure creeping		20	20	20	20	20	0	0	No	No
	Structure lifetime		20	20	20	20	20	0	0	No	No
	dT in-orbit	Struc	-6.34	0.82	-1.8	0.8	0.1	0	0	No	Yes(*)
		refl	7	0	1.6	0	-0.2	-9	-1.9 10-7	No	Yes(*)
	ISMA	Rad	11.1	0	-0.6	0.0	-8.52	6.6	-1.1^{E}-05	No	Yes
		Tang	0.0	-1.4	0.0	0.0	0.0	0.0	0.0^{E}+00	No	Yes
		Out-of-pl	25.4	0.0	-73	0.0	0.	0.8	-1.5^{E}-06	No	Yes
		Rotation	0.0	1.7	0.0	0.0	0.0	0.0	0.0^{E}+00	No	Yes
	ISM B	Rad	-11.1	0	-0.6	0.0	8.52	6.6	-1.1^{E}-05	No	Yes
		Tang	0.0	-1.4	0.0	0.0	0.0	0.0	0.0^{E}+00	No	Yes
		Out-of-pl	25.4	0.0	-73	0.0	0.	0.8	-1.5^{E}-06	No	Yes
		Rotation	0.0	0.9	0.0	0.0	0.0	0.0	0.0^{E}+00	No	Yes
	FEM acc		1	1	1	1	1	1	0	No	No

SR	QM Videogram.		60	0	60	0	196	0	0	Yes	No
	QM T scaling		16	0	10.3	0	70.5	0	0	Yes	Yes(*)
	QM T know		3.4	0	2.1	0	14.9	0	0	Yes	Yes(*)
	CTE non-unif	Frame	-11.7	0	7.4	0	52.6	0	0	Yes	Yes(*)
		Pr pan	-1.1	0	-1.8	0	-1.6	0	0	Yes	Yes(*)
		SR pan	3.2	0	-3	0	-11.6	0	0	Yes	Yes(*)
		Fr st1	0	0	-0.1	0	-0.1	0	0	Yes	Yes(*)
		Fr st2	0	0	-0.1	0	-0.1	0	0	Yes	Yes(*)
		BBS	-0.1	0	-0.2	0	-0.2	0	0	Yes	Yes(*)
		BTS	2.2	0.9	-5.2	-9.9	-18.2	0	0	Yes	Yes(*)
		Sr st1	2.2	0.9	-5.2	-9.9	-18.2	0	0	Yes	Yes(*)
		SR st2	2.2	-0.9	-5.2	10	-18.3	0	0	Yes	Yes(*)
		Low st	0.1	0	0.2	0	0.2	0	0	Yes	Yes(*)
	CS IF load		12.1	0.1	4	0.3	-25.0	0	0	No	No
	Baffle IF load		-10.5	0.0	-18.6	0.1	7.9	0	0	No	No
	FPU IF load		0.5	0.0	1.4	0.0	0.6	0	0	No	No
	PR, SR, JFET		-1.1	0.0	-1.0	0.0	-0.9	0	0	Yes	No
	Gravity release		4.0	0.0	0.6	0.0	-8.5	0	0	No	No
	Moist release	Struc	1.5	0.0	0.5	0.0	-2.7	0	0	No	No
		ref	6.5	0	-0.2	0	-11	1.41	3.3 10-6	No	Yes
	alignment		152	152	152	22.4	22.4	0	0	Yes	No
	CS planarity	E	1.4	0	3.4	0	4.3	0	0	No	Yes(*)
		N-E	-2	-0.6	-2.0	-0.4	0.5	0	0	No	Yes(*)
		N-W	-10.7	-0.8	14.9	29.6	61.0	0	0	No	Yes(*)
		W	-46.9	0	36.1	0	-150	0	0	No	Yes(*)
		S-W	-10.7	0.8	14.9	-29.6	61.0	0	0	No	Yes(*)
		S-E	-2	0.6	-2.0	0.4	0.5	0	0	No	Yes(*)
	TTA	E	0.21	0	0.49	0	-0.35	0	0	No	Yes(*)
		N-E	0.	0.1	0.57	0.8	1.23	0	0	No	Yes(*)
		N-W	-1.9	-0.61	2.51	4.1	9.4	0	0	No	Yes(*)
		W	-7.1	0	4.6	0	-21	0	0	No	Yes(*)
		S-W	-1.9	0.61	2.51	-4.1	9.4	0	0	No	Yes(*)
		S-E	0.	-0.1	0.57	-0.8	1.2	0	0	No	Yes(*)
	Structure launch		20	20	20	20	20	0	0	No	No
	Structure creeping		20	20	20	20	20	0	0	No	No
	Structure lifetime		20	20	20	20	20	0	0	No	No
	dT in-orbit	Struc	8.54	-0.3	5.5	0.6	37.3	0	0	No	Yes(*)
		refl	-3.3	-0.12	-0.7	-0.2	-0.6	4	10-7	No	Yes(*)
	ISM A	Rad	-11.5	0	-1.5	0	-15.5	-2.0	5 E-07	No	Yes
		Tang	0.0	-46	0	0.0	0.0	0.0	0.0^{E}+00	No	Yes
		Out-of-pl	-34	0	60	0	0	0.3	-5.0^{E}-08	No	Yes
		Rotation	0.0	6	0.0	0.0	0.0	0.0	0.0^{E}+00	No	Yes
	ISM B	Rad	11.5	0	-1.5	0	15.5	-2.0	5 E-07	No	Yes
		Tang	0.0	-46	-0.1	0.0	0.0	0.0	0.0^{E}+00	No	Yes
		Out-of-pl	-34	0	60	0	0	0.3	-5.0^{E}-08	No	Yes
		Rotation	0.0	6	0.0	0.0	0.0	0.0	0.0^{E}+00	No	Yes
	FEM acc		1	1	1	1	1	1	0	No	No
FPU	Shimming accuracy		592	413	411	-	-	-	-	No	No
	Stability		400	400	100	-	-	-	-	No	No

(*) PR and SR movements and shape change are correlated
(**) for these load cases, the best focus will be determined, and a refocus will be applied, by shimming the FPU along ZRDP
(***) if yes, the translations and rotations occurs at the same time

For each one of the load cases, a special care is taken to properly consider whether the displacements/distortions are correlated or not between the several axes, and eventually between the secondary and the primary reflectors.

At the center of the field of view, for the 857-1 HIFI horn, the contributions are the following

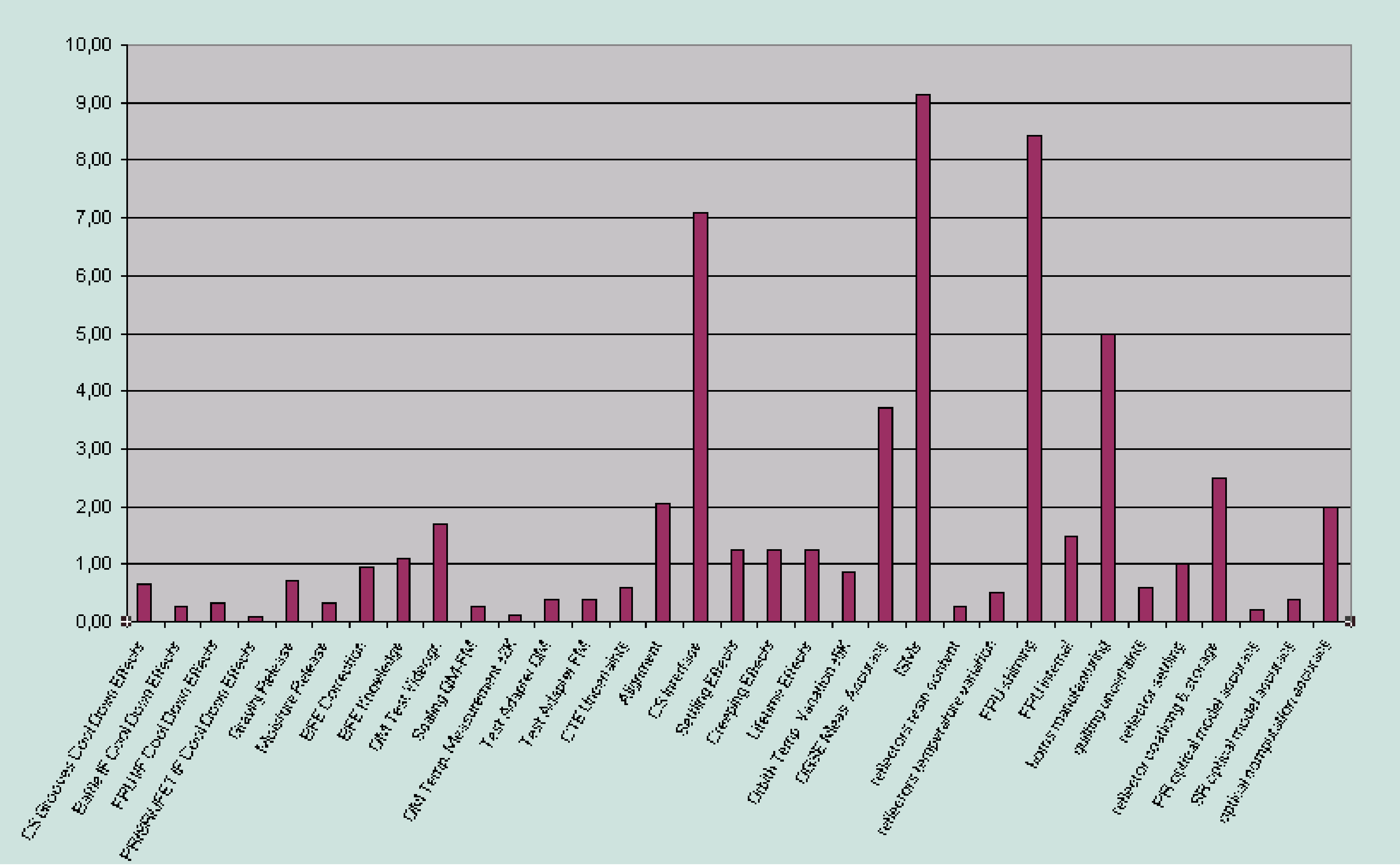

The precedings results call the following comments

Due to the lack of knowledge of the sensitivities of one of the ISM, its contribution has been assessed by multiplying the combination of the two others by 1.5.
Most of the ISM displacements will occur during the FM cryo-test, and will thus be compensated. This has not been considers (at the presented contribution is in this way a worst case) to preserve the coherence between the optical and RF budget
On top of the contributors detailled in (AD5], an allocation of 2µm RMS has been considered for the optical computation accuracy, mainly to cover the way the PR and SR high frequency errors are considered in the model.

On the next page, the random WFE budget is shown on an organigram form, for the 857GHz horn

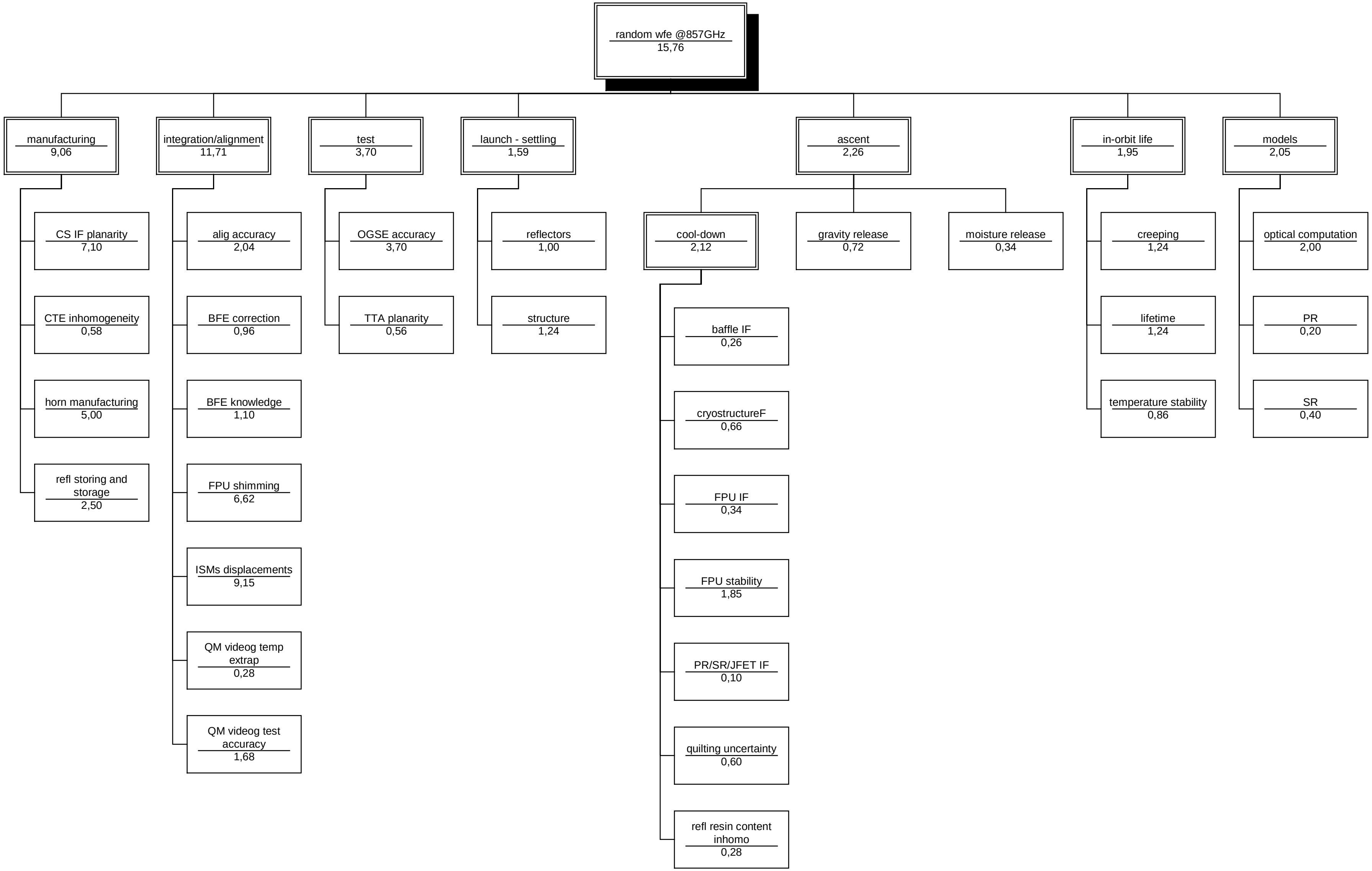
random wfe @857GHz
15,76
manufacturing
9,06
CS IF planarity
7,10
CTE inhomogeneity
0,58
horn manufacturing
5,00
refl storing and storage
2,50
integration/alignment
11,71
alig accuracy
2,04
BFE correction
0,96
BFE knowledge
1,10
FPU shimming
6,62
ISMs displacements
9,15
QM videog temp extrap
0,28
QM videog test accuracy
1,68
test
3,70
OGSE accuracy
3,70
TTA planarity
0,56
launch - settling
1,59
reflectors
1,00
structure
1,24
ascent
2,26
cool-down
2,12
baffle IF
0,26
cryostructureF
0,66
FPU IF
0,34
FPU stability
1,85
PR/SR/JFET IF
0,10
quilting uncertainty
0,60
refl resin content inhomo
0,28
gravity release
0,72
moisture release
0,34
in-orbit life
1,95
creeping
1,24
lifetime
1,24
temperature stability
0,86
models
2,05
optical computation
2,00
PR
0,20
SR
0,40

The analysis at 857GHz horns shows that the uncertainty is driven by what happens at the following interfaces:

- ISMs
- Cryostructure
- FPU

Horns manufacturing (allocation) and performance measurement accuracy contribute a bit less.

The following graphs shows the random WFE for all the horns:

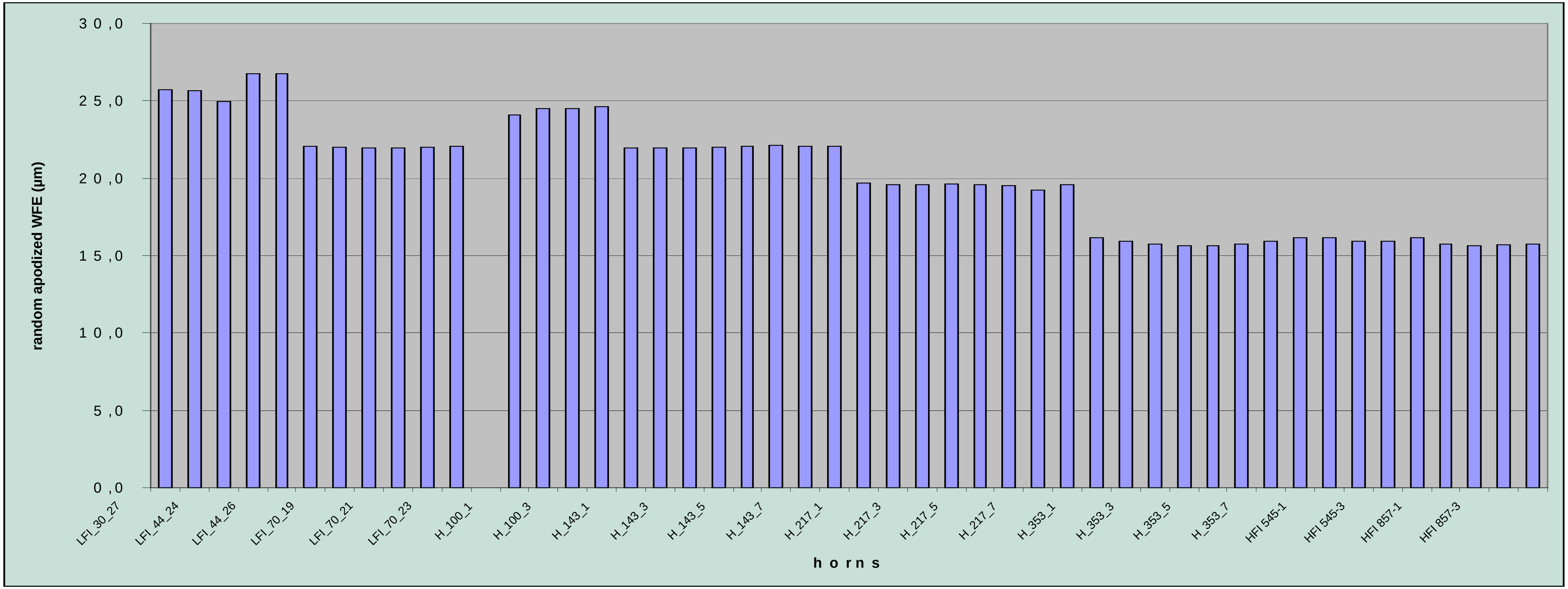

The numbers are given in the next table: (2sigmas)

	Random Apodized WFE (µm)
hfi_100_1	24,1
hfi_100_2	24,5
hfi_100_3	24,5
hfi_100_4	24,6
hfi_143_1	22,0
hfi_143_2	22,0
hfi_143_3	21,9
hfi_143_4	22,0
hfi_143_5	22,1
hfi_143_6	22,1
hfi_143_7	22,1
hfi_143_8	22,1
hfi_217_1	19,7
hfi_217_2	19,6
hfi_217_3	19,6
hfi_217_4	19,6
hfi_217_5	19,6
hfi_217_6	19,5
hfi_217_7	19,2
hfi_217_8	19,6
hfi_353_1	16,2
hfi_353_2	15,9
hfi_353_3	15,8
hfi_353_4	15,6
hfi_353_5	15,6
hfi_353_6	15,8
hfi_353_7	15,9
hfi_353_8	16,2
hfi_545_1	16,2
hfi_545_2	15,9
hfi_545_3	15,9
hfi_545_4	16,2
hfi_857_1	15,7
hfi_857_2	15,6
hfi_857_3	15,7
hfi_857_4	15,8

	Random Apodized WFE (µm)
LFI_30_27	25,7
LFI_30_28	25,6
LFI_44_24	25,0
LFI_44_25	26,8
LFI_44_26	26,8
LFI_70_18	22,0
LFI_70_19	22,0
LFI_70_20	22,0
LFI_70_21	22,0
LFI_70_22	22,0
LFI_70_23	22,1

5.5.3 Complete budget

Linear sum of the deterministic and random case gives the following budget, at all frequencies:

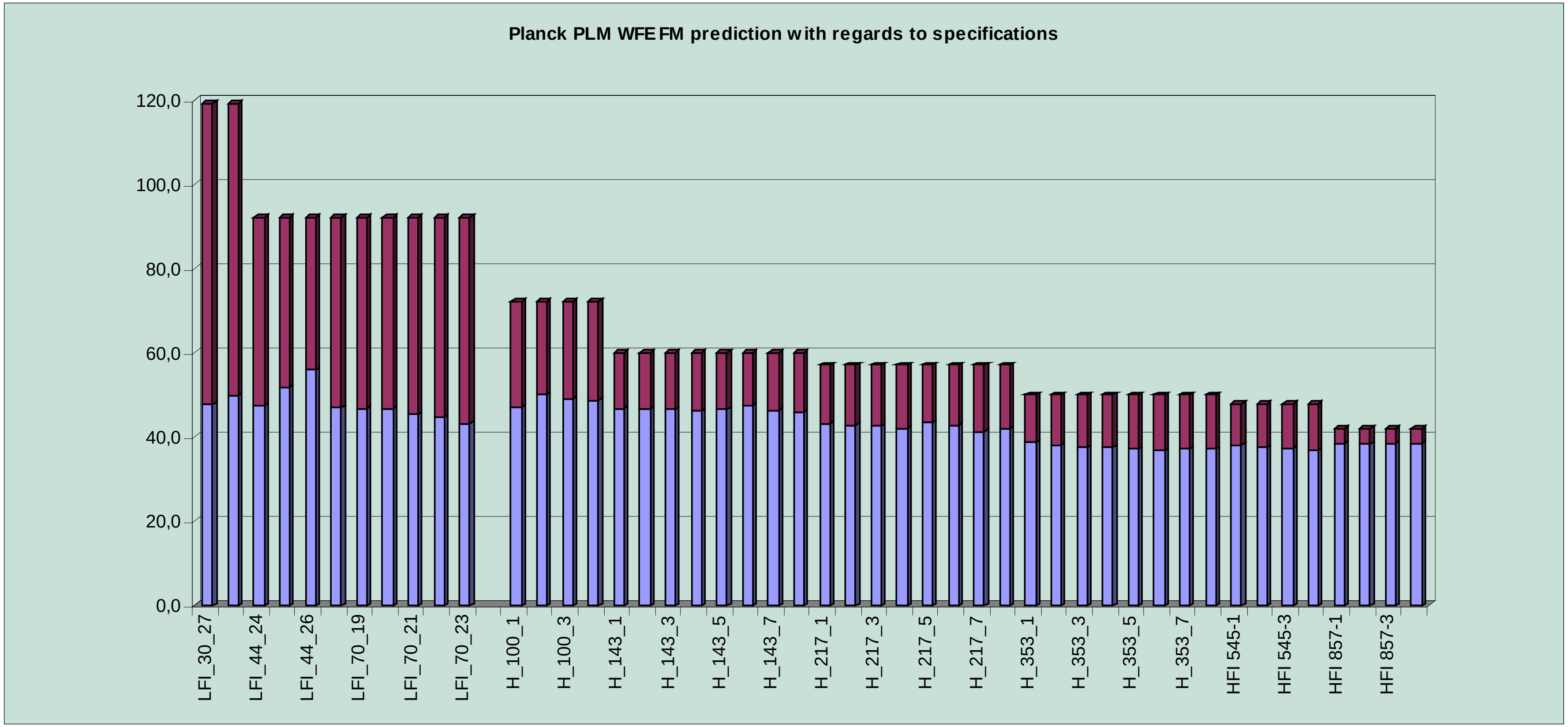

The bottom part of the columns quantifies the budget, whereas the top of top of the columns reaches the specifications. Red part of the column is thus the difference between the budget and the specification.

The following table give the numbers, in µm RMS

horn	Budget (2σ)	specification	Horn	Budget (2σ)	specification
LFI_30_27	47,6	119,0	H_100_1	47,0	72,0
LFI_30_28	49,9	119,0	H_100_2	50,1	72,0
LFI_44_24	47,6	92,0	H_100_3	49,0	72,0
LFI_44_25	51,9	92,0	H_100_4	48,7	72,0
LFI_44_26	56,0	92,0	H_143_1	46,7	60,0
LFI_70_18	47,0	92,0	H_143_2	46,8	60,0
LFI_70_19	46,7	92,0	H_143_3	46,5	60,0
LFI_70_20	46,7	92,0	H_143_4	46,1	60,0
LFI_70_21	45,4	92,0	H_143_5	46,5	60,0
LFI_70_22	44,8	92,0	H_143_6	47,5	60,0
LFI_70_23	43,2	92,0	H_143_7	46,4	60,0
			H_143_8	46,0	60,0
			H_217_1	43,2	57,0
			H_217_2	42,8	57,0
			H_217_3	42,6	57,0
			H_217_4	42,1	57,0
			H_217_5	43,3	57,0
			H_217_6	42,7	57,0
			H_217_7	41,2	57,0
			H_217_8	41,9	57,0
			H_353_1	38,7	50,0
			H_353_2	38,2	50,0
			H_353_3	37,5	50,0
			H_353_4	37,6	50,0
			H_353_5	37,2	50,0
			H_353_6	36,7	50,0
			H_353_7	37,2	50,0
			H_353_8	37,2	50,0
			HFI 545-1	38,2	48,0
			HFI 545-2	37,6	48,0
			HFI 545-3	37,2	48,0
			HFI 545-4	37,1	48,0
			HFI 857-1	38,4	**42,0**
			HFI 857-2	38,3	**42,0**
			HFI 857-3	38,4	**42,0**
			HFI 857-4	38,5	**42,0**

the value at 1 sigma can be compared to the goal

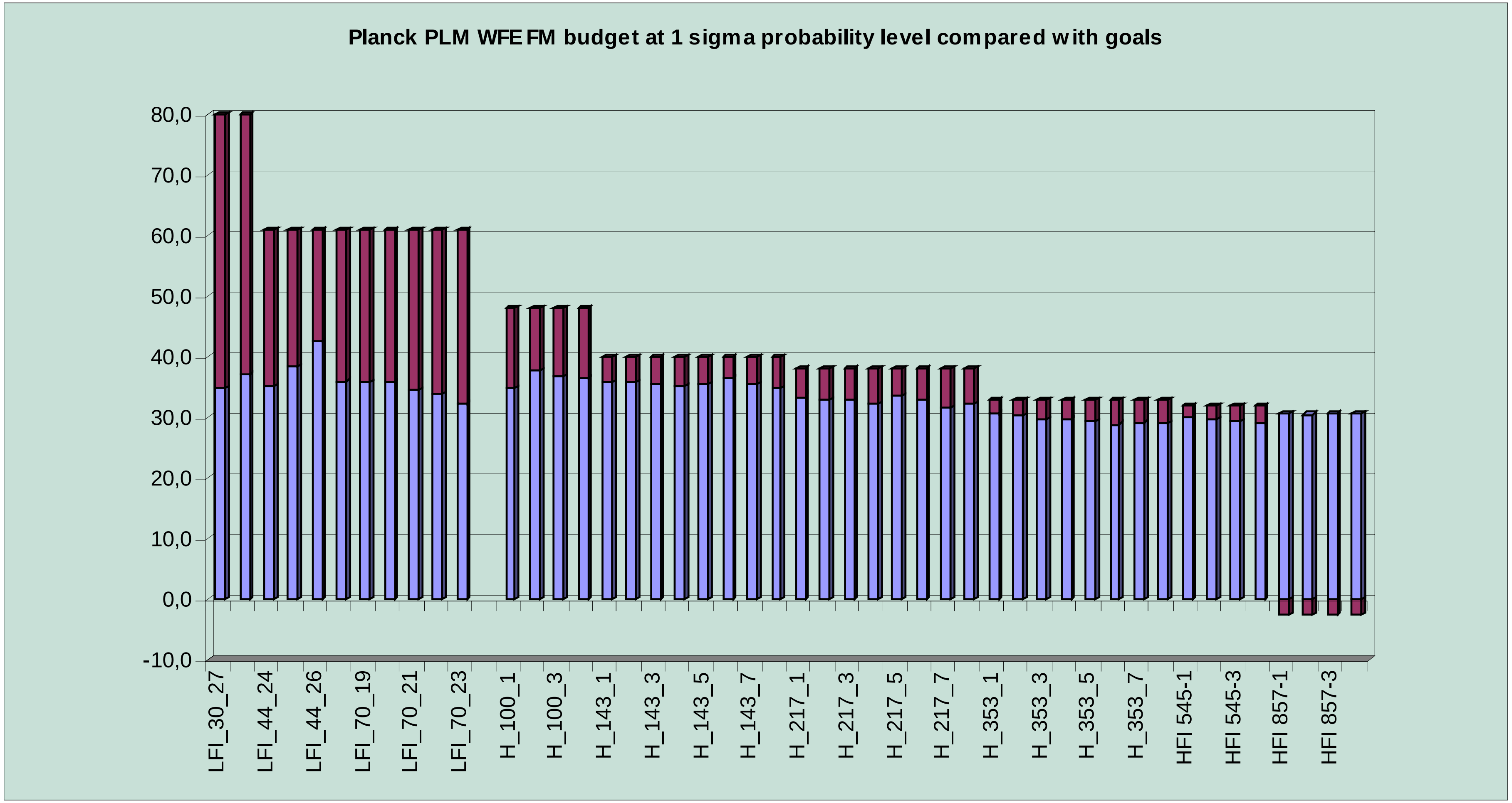

the budget at one sigma slightly exceeds the goal for the high frequency GHz

The following table give the numbers, in µm RMS

horn	budget	specification	Horn	budget	specification
LFI_30_27	34,7	80,0	H_100_1	35,0	48,0
LFI_30_28	37,1	80,0	H_100_2	37,8	48,0
LFI_44_24	35,1	61,0	H_100_3	36,7	48,0
LFI_44_25	38,5	61,0	H_100_4	36,4	48,0
LFI_44_26	42,6	61,0	H_143_1	35,7	40,0
LFI_70_18	35,9	61,0	H_143_2	35,8	40,0
LFI_70_19	35,7	61,0	H_143_3	35,6	40,0
LFI_70_20	35,7	61,0	H_143_4	35,1	40,0
LFI_70_21	34,4	61,0	H_143_5	35,4	40,0
LFI_70_22	33,8	61,0	H_143_6	36,4	40,0
LFI_70_23	32,1	61,0	H_143_7	35,4	40,0
			H_143_8	35,0	40,0
			H_217_1	33,4	38,0
			H_217_2	33,0	38,0
			H_217_3	32,8	38,0
			H_217_4	32,3	38,0
			H_217_5	33,5	38,0
			H_217_6	32,9	38,0
			H_217_7	31,6	38,0
			H_217_8	32,1	38,0
			H_353_1	30,6	33,0
			H_353_2	30,2	33,0
			H_353_3	29,6	33,0
			H_353_4	29,8	33,0
			H_353_5	29,3	33,0
			H_353_6	28,8	33,0
			H_353_7	29,2	33,0
			H_353_8	29,1	33,0
			HFI 545-1	30,1	32,0
			HFI 545-2	29,6	32,0
			HFI 545-3	29,3	32,0
			HFI 545-4	29,0	32,0
			HFI 857-1	30,6	**28,0**
			HFI 857-2	30,5	**28,0**
			HFI 857-3	30,6	**28,0**
			HFI 857-4	30,6	**28,0**

5.6 Statistical considerations

Indeed, at this development stage, WFE is a statistical value. At 857GHz, the apodized WFE has the following distribution law:

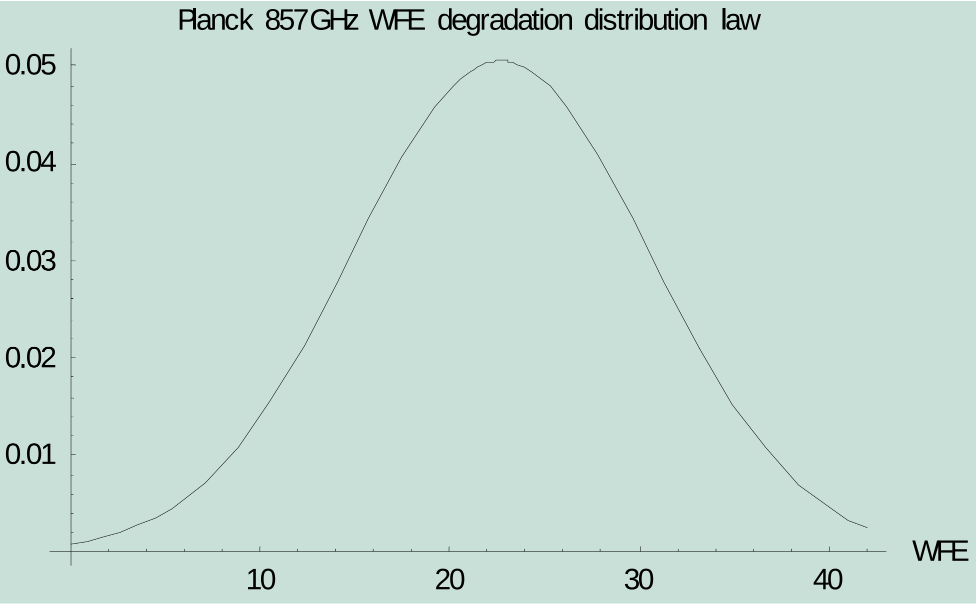

In other words, by integrating the gaussian law, we can conclude in the following way:

- the most probable value for the EOL WFE is the deterministic one: 22.7µm
- there is 68.2% chance that the performance will between 14.8 and 30.6µm
- there is 95.4% chance that the performance will between 6.9 and 38.5µm
- there is 74.9% chance that the performance will meet the goal 28µm
- there is 99.3% chance that the performance will meet the requirement 42µm

6. LINE OF SIGHT

6.1 Definitions

6.1.1 PPLM Line Of Sight definition

The PPLM Line of Sight is defined as the projection on the observed sky of the radiometric center of a detector's far field pattern as projected by the telescope. This direction is referenced with regards to the cryostructure/SVM interface.

The PPLM Around Line of Sight is defined as the orientation of the projection on the observed sky of the radiometric center of a detector's lines far field pattern as projected by the telescope. This direction is referenced with regards to the cryostructure/SVM interface.

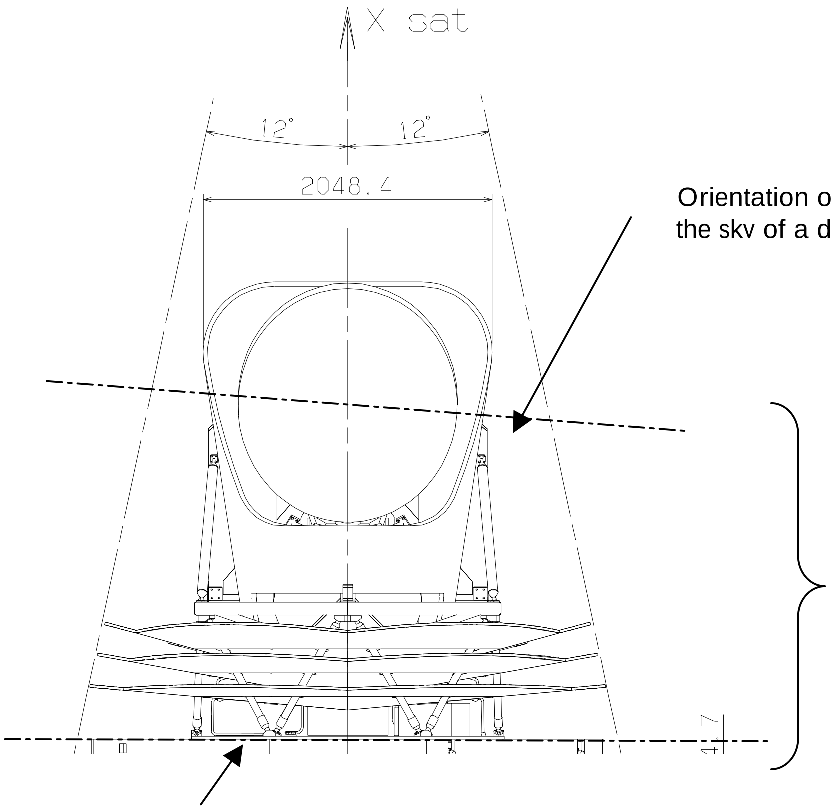

Orientation of the projection in the skv of a detector line:

The angle between these two directions characterizes the Around-LOS angle at PPLM level

P-PLM / SVM interface plane

This definition is derived at Telescope+cryostructure level in the following way

6.1.2 Planck Telescope+cryostructure LoS definition

The Planck Telescope+cryostructure Line of Sight is defined as the projection on the observed sky of the center of the FPU/Telescope Interface, as projected by the actual telescope. This direction is referenced with regards to the cryostructure/SVM interface.

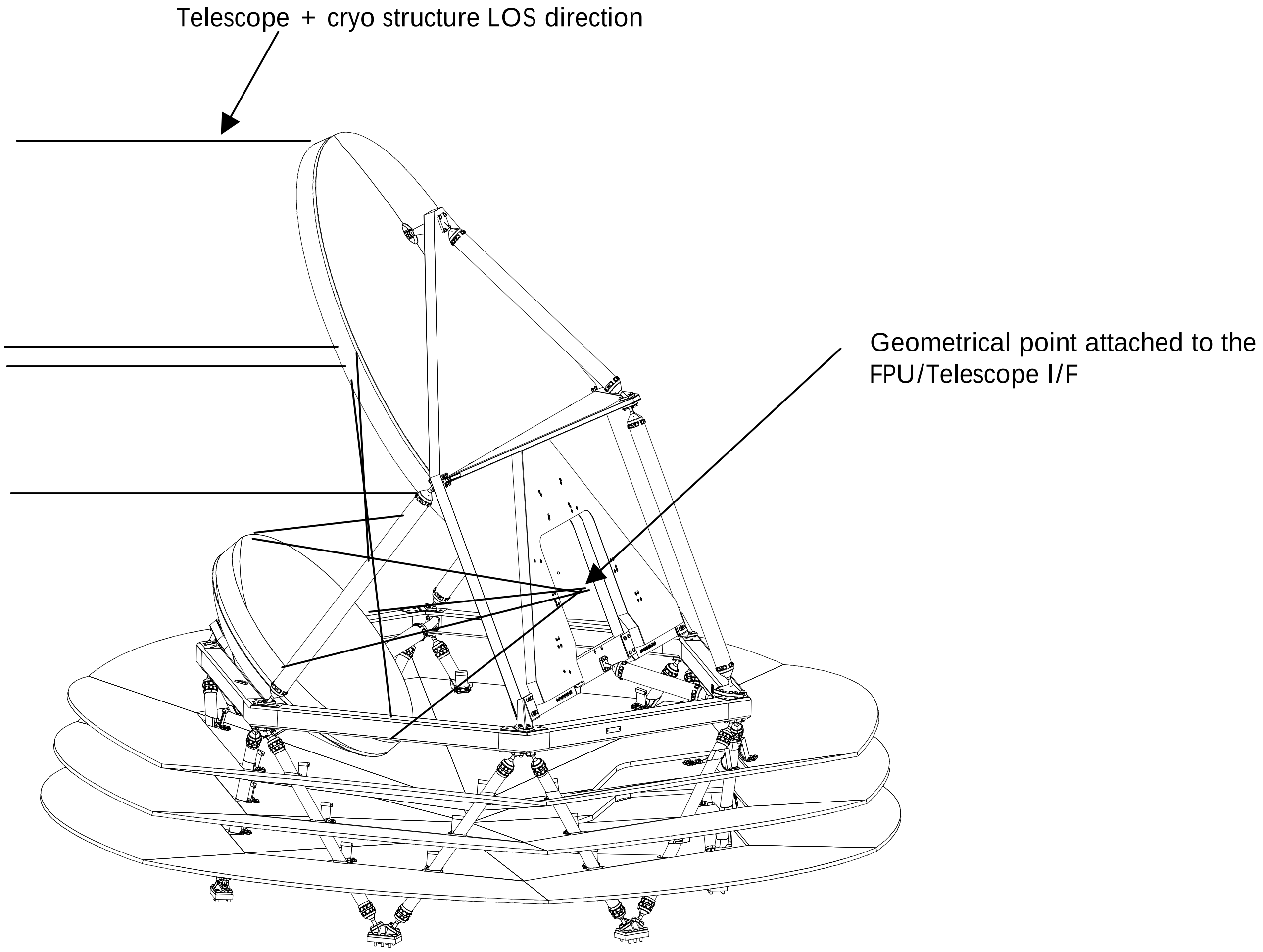

The Planck Telescope+cryostructure around Line of Sight angle is defined as the orientation (with regards to the cryostructure/SVM interface) of projection on the observed sky of FPU/Telescope Interface, as projected by the actual telescope.

6.2 analysis

6.2.1 End of Life LoS direction with regards to P-PLM interface frame

The contributors to the Line of Sight absolute position are the telescope line of sight, the cryostructure, and the instrument line of sight.

6.2.1.1 Telescope line of sight

Contraves, as telescope manufacturer showed that

- the telescope best focus will remain within +/-0.6mm along X with regards to its ideal location(see [RD4]). This correspond to a +/-1.3arcmin.
- the center of the FPU interfaces will remain around –40µm+/-20µm with regards to it's idelal location(see [RD4]). This induces a worst case LOS misalignment of +/-0.13arcmin

6.2.1.2 Cryostructure

The cryostructure is required to have a parallelism between it's two interface planes which shall be better than 0.4mm on a 2400mm diamter interface. This corresponds to a worst case tilt of 0.6arcmin.

6.2.1.3 Instruments contribution

The Panck Alignment Plan [RD1], in annex to the IID-A, asks instruments to provide the following alignment:
The horns must be located (in-orbit) with the following accuracy with regards to the mounting interface to the telescope FPU:

#

+/-0.4mm translation (position and stability) along each X and Y axis, and +/-0.5mrad rotation around each X Y axis

#

Note that there is no budget on the FPU side, so that the PPLM budget is still considering the primary allocations and requirements toward the instruments

Due to the 1600mm telescope focal length, these +/-0.4mm along X correspond to 0.86 arcmin. LoS deviation.

6.2.1.4 LoS budget:

Contributor	**LoS deviation (arcmin)**
Telescope	1.4
Cryostructure	0.6
FPU	0.86
Total	<1.8 arcmin
Alignment need	51

The alignment need is met with margins. This is because the stability is mostly driven by image quality need rather than LOS direction.

6.2.2 P-PLM around LoS stability

The performance mainly depends on the thermal stability of the cryo structure with regards to temperatrure change at the SVM interface. The perfomance is presented in the PPLM design report.

6.2.3 P-PLM around LoS knowledge

The PPLM around LOS knowledge accurcay is given by:

- Horn loction knowledge accuravy at cryo
- Around LOS orientation knowledge of the telescope/FPU IF in cryo
- Measurement accuracy of the location of the FPU – once mounted on th PPLM – with ergards tot he spacecraft cubes.

6.2.3.1 Horns orientation knowledge

In the Planck Alignment Plan [RD1], the instruments are request to provide the following knowledge:

#

Each detector line will have to be known to be aligned parallel to Y axis wrt to telescope/FPU mechanical interface with a 0.33 arcmin accuracy – this has a direct impact on around LOS knowledge.

#

6.2.3.2 FPU cube orientation knowledge

On another hand, the FPU is also requested to provide the following knowledge for it's optical references:

#

The instruments (HFI inside LFI) FPU must be delivered with an alignment cube and optical ball mounted at the rear side.

The location of this optical reference w.r.t the mechanical interface must be known with the following accuracy:

Lateral	0.05mm
Longitudinal	0.05mm
Tilt	20arcsec

This alignment tolls shall be visible at satellite level (with the baffle), as defined in the ID-320 plan.

#

6.2.3.3 Around-Los measurement of the telescope wrt its optical reference

The OGSE develloped by Contraves will measure the location of the telescope focus with an accuracy better than 0.15mm, corresponding to 0.3arcmin

6.2.3.4 Theodolite zaccurcay

Theodolite meaurement will provide us an accuracy better than 10arcsec (2sigma)

6.2.3.5 Budget

The successive knowledge of the preceding contributors leads to the following budget:

Contributor	**Around LoS knowledge (arcmin)**
Horn orientation knowledge	+/-0.33
Telescope around LOS knowledge	+/-0.3
Theodolite accuracy	0.17
Total (RSS)	+/-0.48
Need (see [RD1])	<+/-2 arcmin

The around-LoS knowledge requirement is fulfilled with margins

7. EMISSIVITY

7.1 Requirement

As expressed in [AD1], the requirement on the emissivity of the optical surfaces is the following:
The total emissivity of the telescope optical surfaces < 1% BOL
< 6% EOL
<3% EOL * AT delivery of the telescope

the emissivity increase might come from:
- reflectors coating BOL performance
-reflectors coating ageing
-contamination

7.2 Contributors analyses

7.2.1 Reflectors

The reflectivity is specified in [AD2] in the following way:

PERF-035 : The reflectivity for each reflector and for the frequency range from 25 GHz to1000 GHz and in operating conditions shall be:
- > 0.995 at BOL at delivery of the reflectors
- > 0.975 at EOL, with a goal of > 0.99 at EOL

If we consider that the emissivity e=1-r,, where r is the reflectivity, then we have the following contribution:
1% BOL
5% EOL (goal 2%)

7.2.2 Contamination

7.2.2.1 Molecular contamination

7.2.2.1.1 sources

The following items are molecular contamination sources:
on ground molecular deposition
⇒As justified in the cleanliness End of life Needs techincal note ([RD3]), a worst case approach leads to consider an optical index of n=1.6-0.003i whatever the wavelength.

in-flight material outgassing (Mainly H_2O on cold surfaces <166K)
⇒Water ice thermo-optical data are given in [RD8]

the thermo optical data of water ice at Planck wavelength are:

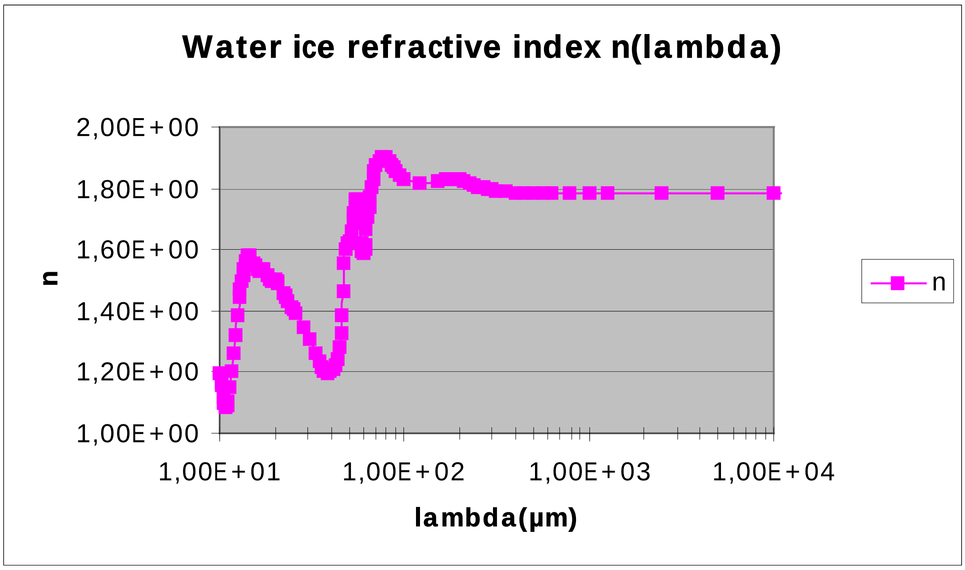

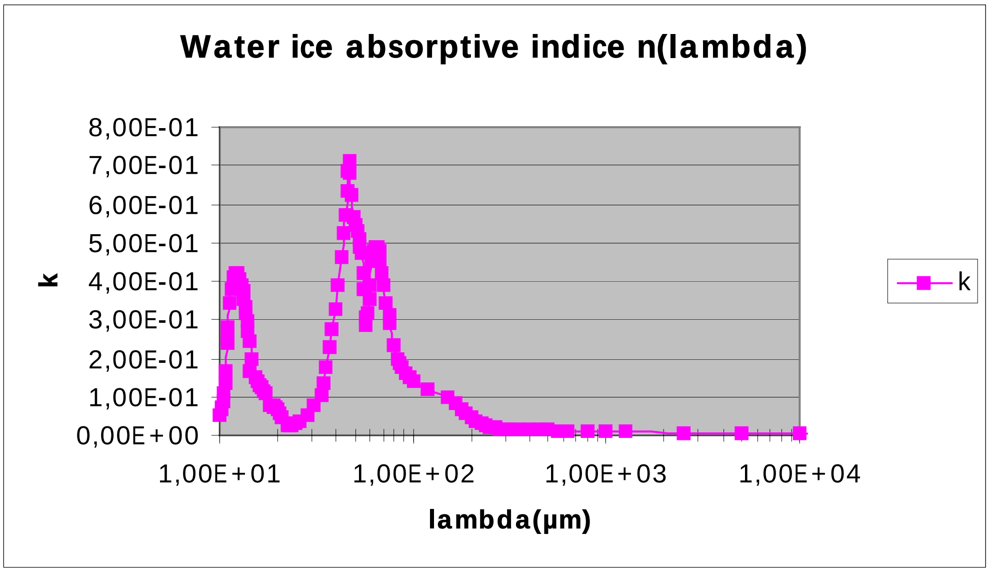

in flight exhaust gas: mainly NH_3 and NH_2 (H_2,H_2O,N_2H_4,$C_6H_5NH_2$ are much less present)

Due to the 70K temperature of the Planck Telescope reflectors, only NH3 will be trapped

⇒Ammonia ice thermo-optical data are given in [RD7]

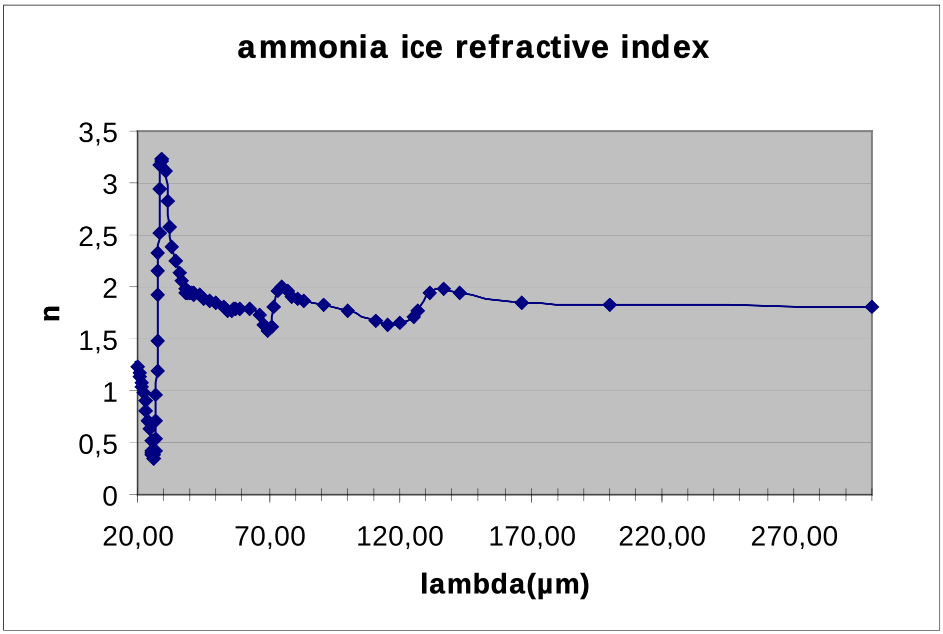

7.2.2.1.2 Prediction

The geometry is the following:

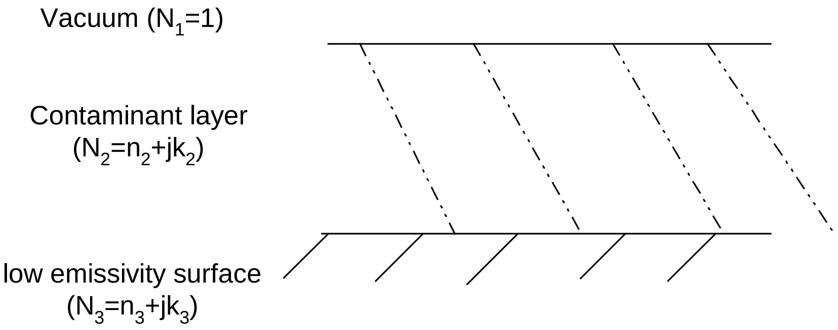

hypotheses

contaminant layer index will is considered as mentionned in the preceding section

Mirror index is considered to be $n_2+jk_2=0.01-150j$

Prediction law

$$\Delta\varepsilon = 1-|r|^2 = 1-\left|\frac{r_{12}+r_{23}e^{2i\alpha t}}{1+r_{12}r_{23}e^{2i\alpha t}}\right|^2$$

Equation 7-1 emissivity change calculation

where : r is the reflection loss on the low emissivity surface

r_{12} is the amplitude reflection loss on the air-contaminant interface

r_{23} is the amplitude reflection loss on the contaminant-mirror interface

$$\alpha = \frac{2\pi}{\lambda} * N_2$$

t is the thickness of the (contaminant) layer

N_2 is the complex index of the (contaminant) layer

is the wavelength

7.2.2.1.3 End of life contamination levels:

Based on the Cleanliness analysis, (cf [RD11]), the maximum amount of contaminants on the reflectors are:

EOL molecular contamination g/cm2.	**H_20**	**NH_3**	**On ground contaminants**
Primary reflector	$5.3\ 10^{-6}$	Neg	$1.08\ 10^{-6}$
Secondary Reflector	$5.9\ 10^{-7}$	Neg	$1.08\ 10^{-6}$

7.2.2.1.4 Emissivity increase assessment

Based on these levels, and on the optical index presented before, the induces emissivity increase is:

EOL emissivity increase	**H_20**	**NH_3**	**On ground contaminants**
Primary reflector	<10-5	0	<10-5
Secondary Reflector	<10-5	0	$<10\text{-}5^{-6}$
total	<10-4		

7.2.2.2 Particulate contamination

7.2.2.2.1 Sources

Particulate contamination might come from

on ground particulate contamination
-clean room
-under fairing
-redistribution

dusting materials (paint)

particle redistribution
-during launch phase
-during S/C reorientation phases

micrometeoroids

7.2.2.2.2 Prediction

A particle emissivity of 0.8 has been considered. This is a slightly worst case. Considering a perfect thermal coupling between the surface and the particle (this is realistic), we have the following relationship:

Particulate contamination level	300ppm	1000ppm	5000ppm	10000ppm
Emissivity increase	0.00024	0.0008	0.004	0.008

7.2.2.2.3 End of life contamination levels

According to the cleanliness requirements specification [RD11], the maximum allowed particulate contamination level is 5000ppm on each reflector.

7.2.2.2.4 Emissivity increase assessment

The emissivity increase due to particulate contamination is 0.004 per reflector, i.e. a total of 0.008

7.2.2.3 Contingency

A contingency of 0.002 emissivity increase is considered at this stage of the project, to cope with any refinement of the hypotheses on contamination impact assessment.

7.3 Complete budget

Contributor		**Stage**	**Total emissivity %**
Reflectors		BoL	1
		EoL (goal)	5(2)
System contamination	Molecular	EoL	<10-2
	particulate	EoL	0.8
	contingency	EoL	0.2
Total		**EoL(goal)**	**6(3)**

7.4 Conclusion

The required 6% are just met, considering a system contigency of 0.2. The reflectors are the main contributors

END OF DOCUMENT